

1 **The 1538 eruption at Campi Flegrei resurgent caldera: implications for future unrest and**
2 **eruptive scenarios**

3 **Giuseppe Rolandi¹, Claudia Troise², Marco Sacchi³, Massimo di Lascio⁴, Giuseppe De Natale²**

4 ¹ Retired Professor at Università di Napoli Federico II, Dept. Earth Sciences, Naples (I)

5 ² Istituto Nazionale di Geofisica e Vulcanologia, Osservatorio Vesuviano, Naples (I)

6 ³ ISMAR-CNR, Naples (I)

7 ⁴ Free Lance Geologist, Naples (I)

8 Corresponding author: Giuseppe De Natale, giuseppe.denatale@ingv.it

9

10

11 Abstract

12 The recent unrest in the Campi Flegrei caldera which began several decades ago, poses a high risk to
13 a densely populated area, due to significant uplift, very shallow earthquakes of intermediate
14 magnitude and the potential for an eruption. Given the high population density, it is crucial, especially
15 for civil defense purposes, to consider realistic scenarios for the evolution of these phenomena,
16 particularly seismicity and potential eruptions. The eruption of 1538, the only historical eruption in
17 the area, provides a valuable basis for understanding how unrest episodes in this caldera may evolve
18 toward an eruption. In this paper, we provide a new historical reconstruction of the precursory
19 phenomena of the 1538 eruption, analyzed considering recent volcanological observations and results
20 obtained in the last few decades. This allows us to build a coherent picture of the mechanism and
21 possible evolution of the present unrest, including expected seismicity, ground uplift and eruptions.
22 Our work identifies two main alternative scenarios, providing a robust guideline for civil protection
23 measures, and facilitating the development of effective emergency plans in this highly risky area.

24 **1. Introduction**

25 The Campi Flegrei area has been a benchmark of modern geology and volcanology since the middle
26 XVIII century, due to the clear evidence of significant ground movements, associated with both uplift
27 and subsidence, imprinted on the columns of the ancient Roman Market (Macellum; hereafter also
28 called Serapeum or Serapis Temple) in the town of Pozzuoli. These movements were famously
29 depicted on the cover of Charles Lyell's seminal book, 'Principles of Geology'. By the XIX century,

30 it became evident that the impressive relative movements between sea level and ground were due to
31 ground uplift and subsidence. Consequently, numerous efforts have been made to reconstruct the
32 timeline of these movements, during the centuries. One of the most convincing reconstructions was
33 proposed by Parascandola (1947), later modified by Dvorak and Mastrolorenzo (1991), Morhange et
34 al. (2006), Bellucci et al. (2006) and, more recently, Di Vito et al. (2016). However, all these
35 reconstructions exhibit evident discrepancies, and do not rely on the full body of historical evidence,
36 as we will demonstrate. These significant ground movements have predominantly involved a long-
37 term trend of subsidence, punctuated by occasional episodes of rapid ground uplift, culminating in
38 the only eruption occurred in historical times, in 1538 (Di Vito et al., 2016). After the 1538 eruption,
39 a new period of subsidence began, which was interrupted in 1950, when a new series of uplift episodes
40 commenced (Del Gaudio et al., 2010). Two major uplift episodes occurred between 1969-1972 and
41 1982-1984, characterized by significant and rapid uplift (with a cumulative uplift of about 3.5 m)
42 accompanied by intense seismicity. These events led to the evacuation of 3000 residents from the
43 oldest part of Pozzuoli town (Rione Terra), in 1970, and the entire town of Pozzuoli comprising
44 40.000 people, in 1984 (Barberi et al., 1984). After approximately 20 years of subsidence, a new
45 uplift phase began in 2005-2006, with a much lower uplift rate (less than 0.01 meters per month on
46 average, compared to about 0.06 meters per month in the 1970s and 1980s), but long-lasting and still
47 ongoing. This new unrest has been accompanied by progressively increasing seismicity, which has
48 substantially intensified, both in frequency and maximum magnitude (Troise et al., 2019; Iervolino
49 et al., 2024). The maximum magnitude reached $M=4.4$ on May 20, 2024, once the maximum ground
50 level attained at the end of 1984 was reached (in July 2022) and surpassed. The progressively
51 increasing seismicity confirms the predictions of Kilburn et al. (2017) and Troise et al. (2019), who
52 based their forecast on the correspondence of the ground level with stress levels at depth. This seismic
53 activity represents a significant and continuous hazard for the edifices in such a densely populated
54 area, given the very shallow depth of the earthquakes (about 2-3 km). Furthermore, the current crisis
55 poses an even higher threat as it could potentially be a precursor to a future eruption in the area.

56 The present study is aimed to reconstruct and interpret the events before and after the 1538 eruption.
57 This analysis follows three main paths: i) the accurate reconstruction, of the ground movements in
58 this area since early historical times, using historical testimonies and documentation; ii) the accurate
59 reconstruction of the uplift movements that evolved from 1430 to 1538, accompanied and followed
60 by significant seismic events; iii) the analysis of stratigraphic and geophysical parameters, which,
61 although collected in the recent era, provide important elements for the reconstruction and
62 interpretation of the unrest related to the 1538 eruption.

63 Finally, the interpretation of the events preceding, accompanying and following the 1538 eruption is
64 used to provide insight into possible evolution scenarios for the present unrest, which started in 1950
65 and is still in progress (Troise et al., 2019; Scarpa et al., 2022)

66

67 **2. Caldera formation and post-caldera volcanic activity 14 ka - 3.7 ka**

68 Campi Flegrei is an active caldera to the west of Naples in southern Italy. About 12-14 km
69 across, its southern third is submerged beneath the Bay of Pozzuoli. Following the most
70 recent, and likely only (Rolandi et al., 2020a; 2020b; De Natale et al., 2016), episode of
71 caldera formation, i.e. the Neapolitan Yellow Tuff eruption 15 ka, some 70 eruptions (linked
72 to 35 visible vents) have occurred across the caldera floor, ranging from the effusion of lava
73 domes to explosive hydro-magmatic eruptions (Di Vito et al., 1999; Smith et al., 2011; Isaia
74 et al., 2015). The most recent eruption occurred in 1538, producing the cone of Monte Nuovo
75 (Di Vito et al., 1987; 2016). The caldera collapse resulted in many new fractures, which
76 gradually became eruptive vents. Through these vents, the eruptions continued, exhibiting
77 the characteristics of a volcanic field (Druitt and Sparks, 1984), resulting in the so-called
78 post-caldera activity. Dome-shaped uplift of NYT occurred after the caldera formation in the
79 central zone of Campi Flegrei, with uplift up to hundreds of meters on the caldera floor (Rolandi
80 et al., 2020b). The significant uplift involved a large intra-calderic NYT block, making Campi Flegrei
81 a typical example of resurgent caldera (Luongo et al., 1991; Orsi et al., 1996; 1999; Acocella (2010);
82 Rolandi et al., 2020b). The post-caldera activity gave rise to numerous craters, predominantly
83 tuff cones and tuff rings (Fig. 1a,b), displaying the typical characters of monogenic
84 volcanoes (Marti et al., 2016). Within Campi Flegrei, 35 small eruptive centers have been
85 identified, since the NYT eruption (Di Vito et al., 1999; Smith et al., 2012), producing about
86 70 eruptions. The magmas associated with these eruptions are typically trachytes and alkali
87 trachytes, with smaller amounts of latite and phonolite (Di Girolamo et al., 1984; Rosi and
88 Sbrana, 1987; D'Antonio et al., 1999). The post-caldera eruptions can be then classified
89 in two periods, occurring between 14 ka and 8.2 ka BP and 5.8 and 3.7 ka BP., respectively,
90 with an interval of significant subsidence without eruptions from 8.2 to 5.8 ka BP
91 (Rolandi et al., 2020b).

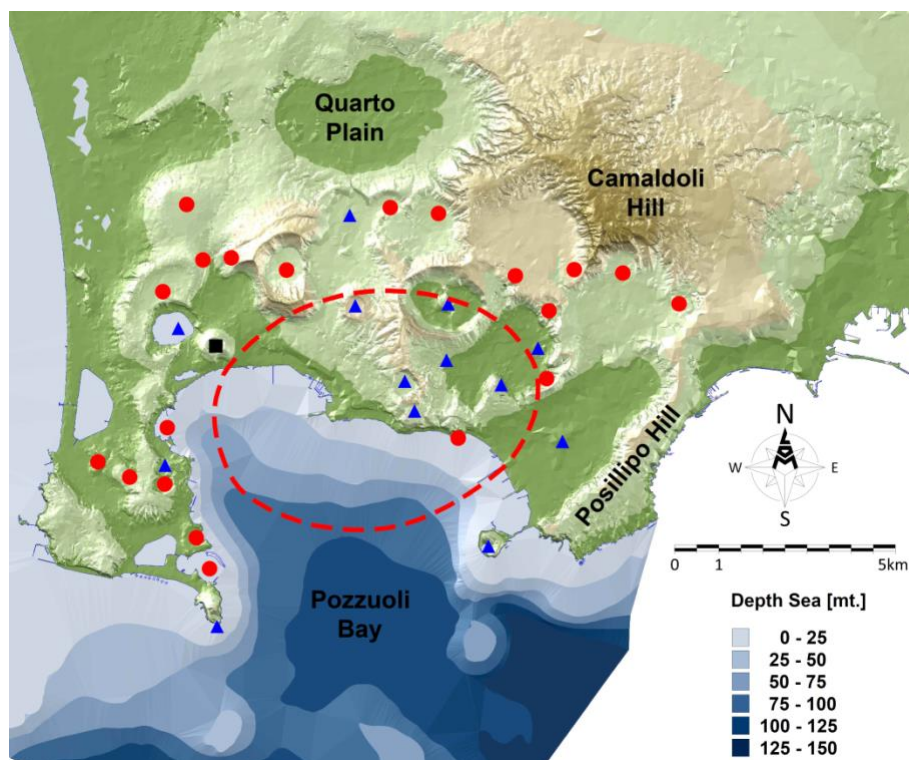
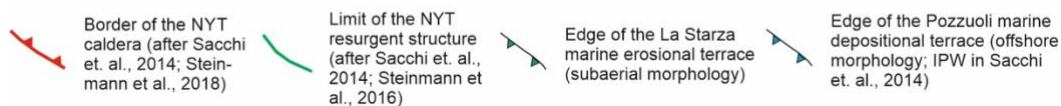
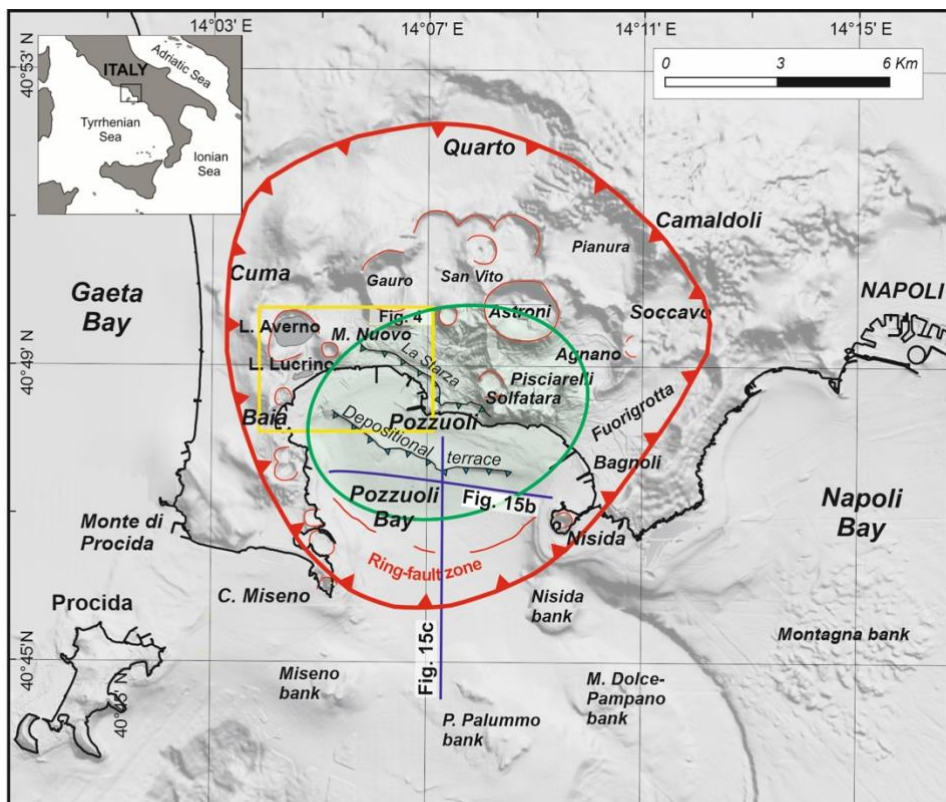


Fig. 1 – Top: Location map of the study area with indication of relevant toponyms and major volcano-tectonic and morpho-structural lineaments associated with the Campi Flegrei caldera. **Bottom:** Map of Campi Flegrei caldera. Red circles indicate the craters of the first post-caldera volcanic phase, blue triangles indicate the craters of the second phase. The red hatched area represents the resurgent block of NYT extended in the Pozzuoli Bay.

100 The second post-caldera eruptive phase was preceded by the uplift of 30m, above sea
101 level, of La Starza marine terrace (Cinque et al., 1983; Rolandi et al., 2020b). The
102 distribution of eruptive centers reveals that, during the first post-caldera phase, they were
103 distributed around the resurgent block. In the second phase, among thirteen volcanic edifices,
104 seven occurred within the resurgent area (Fig. 1).

105 It seems likely that the second post-caldera phase (5.8 - 3.7 ka) can be considered the primary
106 reference for defining possible future eruptive scenarios, following the eruption of 1538 AD.

107

108 **3. Subsidence and uplift evolution before the 1538 eruption**

109 **3.1 Previous interpretations**

110 Modern research on ground movements at Campi Flegrei caldera started with the detailed
111 studies by Parascandola (1943; 1947), the latter drawing mainly on earlier work by Niccolini
112 (1846). The 1943 study primarily focused on historical documents describing the
113 subsidence of the ancient Greek-Roman road known as ‘Via Herculea’, which was located
114 near the Averno volcano, and contributed to the formation of Lake Lucrino.

115 The Via Herculea, in use since Greek times (beginning in the 8th century BC) and remaining
116 important throughout the Roman times, serves as fundamental historical marker for
117 assessing ground movements west of Pozzuoli. The detailed history of this road,
118 reconstructed from numerous historical sources and included in the supplementary material,
119 provides insights into its subsidence over the centuries.

120 The road ran along a narrow strip of land, likely formed by coastal aggradation of
121 volcanoclastic sandy deposits (Parascandola, 1943) primarily from the 5 ka and 3.7 ka
122 eruptions of the Averno and Capo Miseno volcanoes (Insinga et al., 2006; Di Vito et al.,
123 2011; Sacchi et al., 2014; Di Girolamo et al., 1984), which eventually created a lake (Fig.
124 2a). Given its elevation just a few meters above sea level, subsidence significantly affected
125 its usability, with frequent disruptions documented in historical records. These records
126 provide crucial evidence of the evolution of ground subsidence in this area over the
127 centuries.

128 The Greeks arriving from Euboea in the 8th century BC, initially settled on the island of
129 Ischia (Pithecura), before founding the polis of Cuma, the first Greek colony in Magna
130 Graecia and the entire western Mediterranean. From this time the narrow land strip served
131 as a road known as the Via Herculea, providing access to the cultivated countryside around
132 Pozzuoli (Fig. 2b).

133 Parascandola (1943) emphasized the continuous subsidence of the Via Herculea, using
134 historical accounts from Petrarca (1341) and Boccaccio (1355-1373) to establish that the
135 road had already sunk below sea level by their time. He also noted that Via Herculea did not
136 re-emerge during the uplift accompanying the 1538 eruption, suggesting that the ground
137 uplift in this area was insufficient to compensate for the secular subsidence.
138 In his later work, Parascandola (1947) presented a detailed reconstruction of ground
139 movements in Pozzuoli, based on evidence fundamental reference for subsequent studies on
140 this subject. According to Parascandola (1947) the maximum subsidence occurred during
141 the IX century.
142 The first paper to propose an alternative model for ground movements at Campi Flegrei was
143 published by Dvorak and Mastrolorenzo (1991). They propose simplified and constant rates
144 of subsidence and uplift, suggesting that the maximum subsidence occurred at the end of
145 15th century.
146 Morhange et al. (1999; 2006), based on radiocarbon dating of lithodome shells, identified
147 an additional episode of ground uplift between 650 and 800 AD. Bellucci et al. (2006) later
148 integrated the ground deformation model of Dvorak and Mastrolorenzo (1991) with the
149 findings of Morhange et al. (1999; 2006) into a unified framework.
150 More recently, Di Vito et al. (2016) proposed a new reconstruction of ground movements,
151 which will be discussed in more detail in the following paragraphs. Their model suggests that
152 the maximum subsidence occurred in 1251 AD. They also hypothesized that subsidence at
153 Campi Flegrei began around 35 BC, and that the ground at the Monte Nuovo vent uplifted by
154 approximately 19 meters immediately before the 1538 eruption.

155

156 **3.2 Reconstructing the ground movements with the whole available data set**

157 As inferred from historical chronicles, as well as from studies on the incrustations and traces of
158 bioerosion on the Pozzuoli Serapeum marble columns (Parascandola 1947; Bellucci et al. 2006), after
159 the two post-caldera phases previously defined, large ground uplift and subsidence in the order of
160 tens of meters occurred. Historical documents allowed us to precisely reconstruct such ground
161 movements in Pozzuoli area (central part of the caldera) and in the Averno area (3 km west of
162 Pozzuoli, close to the area where the 1538 eruption occurred. The reconstruction reported here, based
163 on all reliable historical documents, is the most complete and rigorous, allowing to put strong
164 constraints on the reconstruction of past ground movements, whose interpretation is presently very
165 unconstrained and hence variable among the different authors..

166

167 3.2.1 Ground movements at Averno

168

169 The first evidence of subsidence in the Campi Flegrei area dates back Greek times, as reported by
170 Diodoro Siculo (VIII century BC) and is related to the area in front of the Averno Lake, and of the
171 1538 eruption which generated the Monte Nuovo cone. We will start to describe the historical
172 documents to shed light on the ground movements in this area, then we will reconstruct ground
173 movements in the most deformed, central Pozzuoli area.

174 A fundamental historical marker for inferring the ground movements west of Pozzuoli, as already
175 mentioned, is the Via Herculea. Diodoro Siculo (see Appendix 1) reported that, already at the times
176 of first Greek settlements, i.e. 8th century BC, continuous subsidence affected this area, thus
177 generating problems to the practicability of Via Herculea.

178 In Roman times, since the beginning of the 1st century BC, the body of water enclosed by the Via
179 Herculea, purchased by Sergio Orata, played an important role in fish-farming since 90 BC, taking
180 the name of Lucrino, much larger than the present-day Lake Lucrino. After his death, due to
181 continuous subsidence which menaced both the practicability of the Via Herculea and the fish farming
182 activities, the new owners around 50 BC turned to the Roman Senate calling for appropriate
183 interventions. For this purpose, in the period 48-44 BC Julius Caesar was commissioned, then
184 building a barrier (*Opus Pilarum*) and special shutters to protect the road and the Lucrino Lake from
185 sea ingression (see Appendix 1). Towards the end of the same century, for military purposes, in 37
186 BC Agrippa cut both the Via Herculea and the barrier with the crater of Avernus. Having understood,
187 unlike Julius Caesar, the continuous subsidence of the Via Herculea, which at the end of the century
188 was only few meters above sea level (Fig. 2c), Agrippa also **increased its height** (Strabo, 1st century
189 BC). About four centuries later, Theodoric (King of the Ostrogoths), upon request for the protection
190 of fish farming, restored the dam by increasing again the height of via Herculea with respect to the
191 sea level (Parascandola, 1943).

192 Due to continuous subsidence, the Via Herculea finally sank below the sea level between 6th - 7th
193 century A.D, when the sea penetrated the crater of Averno, the Lake Lucrino having disappeared (Fig.
194 2d). Proof of the disappearance of the Via Herculea and of the Lucrino Lake was also testified by
195 Boccaccio, who lived in the Naples area from 1327 to 1341 AD and described the Averno area in its
196 geographical book 'De montibus' (...to Avernus, connected in ancient times with the nearby lake
197 Lucrino where it recalls the waters of portus Iulius).

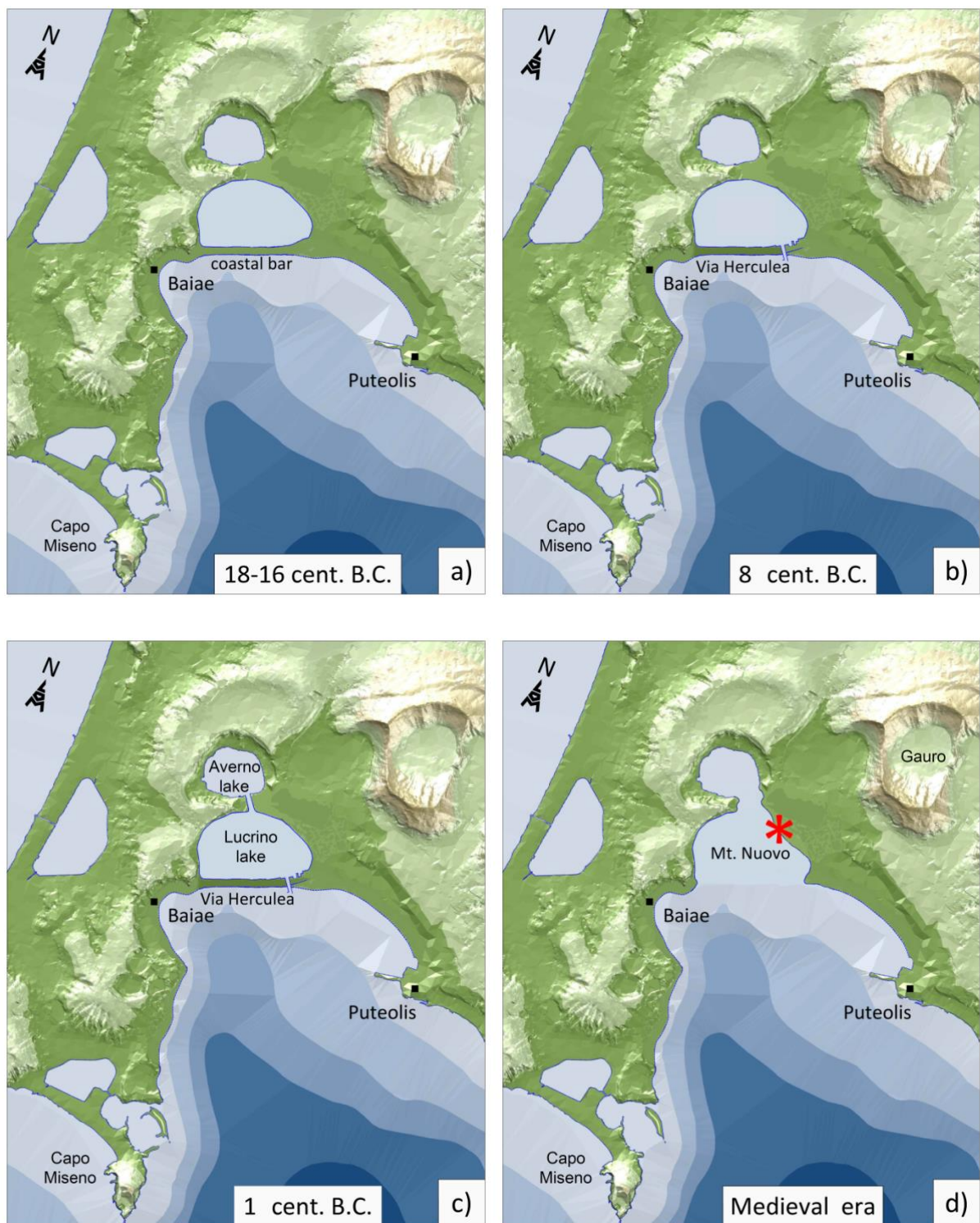
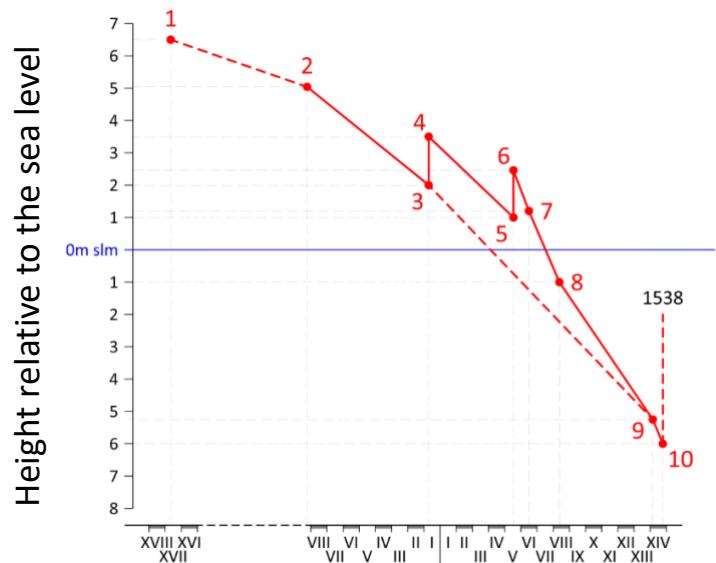


Fig. 2 - a,b,c,d) position and shape of the via Herculea, Lucrino and Averno lakes, along 33 centuries. The red star indicates the central point around which the volcanic edifice of 1538 was formed.

Via Herculea never rose above the sea level again, despite the large uplift phase occurred before and during the 1538 eruption (see Fig. 2d).

206 The tentative reconstruction of the level of Via Herculea, approximately shown in Fig. 2 as briefly
 207 described above, is shown in detail in Fig. 3, where each point of the curve refers to a specific
 208 documented historical period, starting from the Greek age (8th century BC), through the Roman era
 209 and the late Middle Ages, until the eruptive event of 1538 (see Table 1, and Appendix 1). Note that
 210 on the Via Herculea, at the end of the 1st century BC and at the end of the 4th century AD, works
 211 were carried out to increase its height above sea level due to the incipient submersion. Due to these
 212 works, the submersion of the structure was delayed from ca. the 3rd, 4th century BC, up to the 7th
 213 century AD (Fig. 3). The date of submersion around 6-7th century is also consistent with the
 214 observations reported by Parascandola (1943), indicating that the land strip of Via Herculea still
 215 emerged above sea level for much of the 6th century.
 216 It is fundamental to note that Via Herculea never emerged again, not even immediately before and
 217 during the eruptive phase of 1538 (Parascandola, 1943).
 218 The submerged relicts of the Via Herculea are still visible today, located at about 4.5 meters bsl, as
 219 shown in the high-resolution bathymetry (Fig.4) recently obtained by Somma et al. (2016).

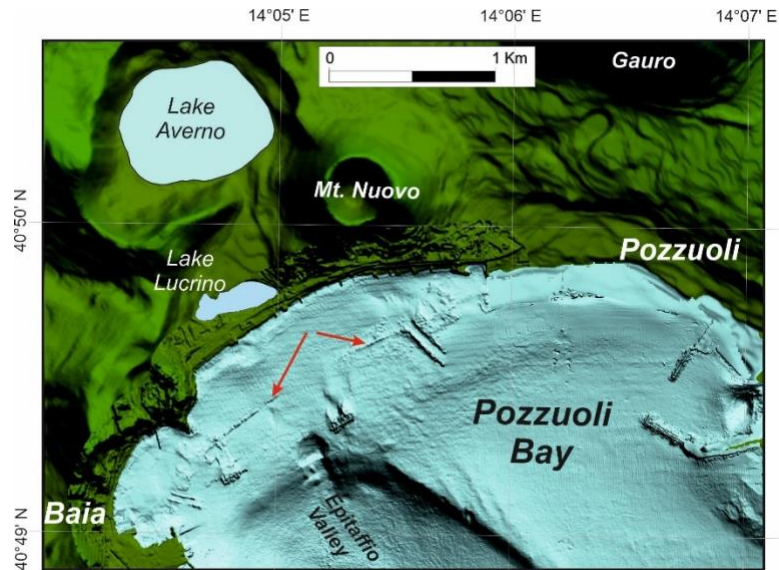


231 **Fig. 3 – Diagram showing the trend of ground movements at the Via Herculea, as referred to sea level,**
 232 **along 33 centuries. Numbers on the curve indicate the times of references for the inferred level:**
 233 **they are synthetically reported in Table 1 and extensively explained in Appendix 1. Dashed lines**
 234 **represent hypothesized subsidences: the first one connecting to the likely initial elevation, the second**
 235 **one showing the likely subsidence path in absence of the restoration works (points 4 and 6), the third**
 236 **one showing the likely uplift linked to 1538 eruption.**
 237

Number	Time	Event	Reference source	Reported by
1	3.7 ka and after	Formation of the coastal bar	This paper	
2	8 th century BC	Subsidence of the via Herculea	Diodorus Siculus (Book IV)	Parascandola, 1943

3	60 BC	Sergio Orata, owner of the 'Lucrino' lake fish farm, asked the Senate to have via Herculea repaired, because at around 2 m asl. Cesare repaired it	Parascandola, 1943	
4	37 BC	Agrippa raised the level of via Herculea	Strabone	Parascandola, 1943
5	12 BC	Abandonment of Portus Julius and Lucrino fish farming, because of accelerated subsidence of via Herculea	Aucelli, 2020	
6	496 AD	Theodoric, King of Gotes, repaired and raised level of via Herculea	Cassiodorus, Varia Book I	Parascandola, 1943
7-8	556 AD	Failed attempts to restore fish farming in the Lucrino lake: the level of Dam was too low	Parascandola, 1943	
9	1341-1348	Petrarca and Boccaccio writings indicate via Herculea was about 5-6 m bsl	Boccaccio, 1355-1373	Parascandola, 1943
10	15 th century	Uplift starts, but Lucrino lake however disappeared and via Herculea never re-emerged	Several chroniclers of the time	Parascandola, 1943

Table 1 - Sinthetic sketch of the main historical sources used to reconstruct the ground deformations shown in Fig.3 (see Appendix 1 for more details).



244 **Fig. 4 – Shaded relief map of the coastal area of the Pozzuoli Bay based on high resolution**
245 **multibeam bathymetry (Somma et al., 2016). Arrows indicate the submerged remains of the**
246 **breakwater pilae of the via Herculea.**

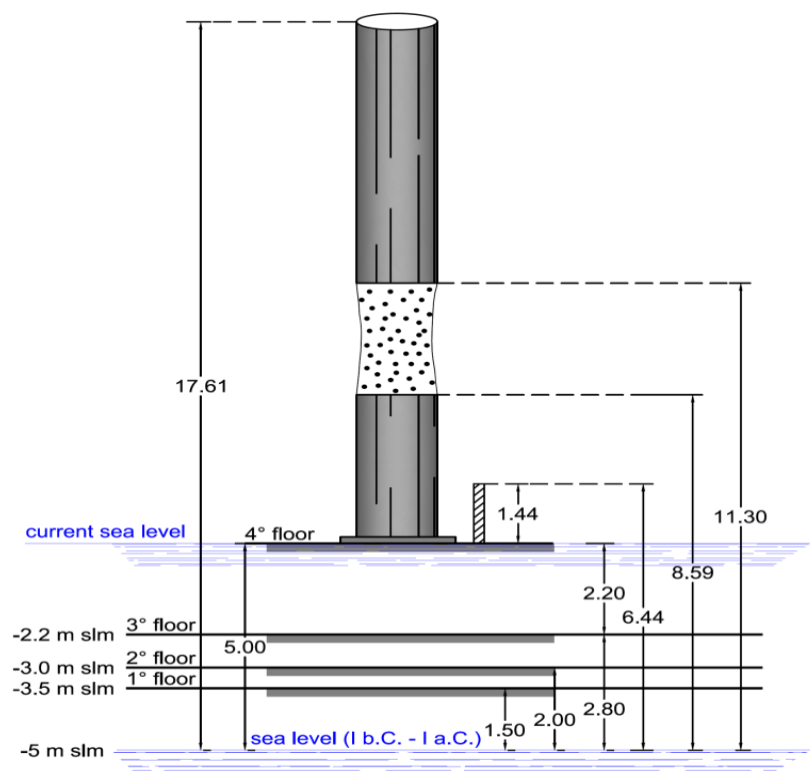
247

248 **3.2.2 Ground movements at Pozzuoli**

249

250 Meanwhile Via Herculea records the most ancient subsidence in the whole area, the best evidence for
251 subsidence in the Pozzuoli area, where maximum ground movements are recorded, comes from the
252 historical-archaeological elements linked to the Serapis Temple (Macellum), although subsidence in
253 the Pozzuoli area is also testified since Greek times (Gauthier, 1912).

254 Recently, Amato and Gialanella (2013) discovered, by drilling into Serapeum area, four successively
255 superimposed floors, ranging from the Augustan age (31 BC-14 AD) to that of the Severi (193-235
256 AD), thus indicating the progressive subsidence of the manufact (Fig. 5). The most elevated 4th floor
257 was built in the Severi Age, indicating at that time the previously built three floors were all below
258 the sea level, and from this epoch we will follow the historical traces of further subsidence and
259 subsequent uplift. The resulting time evolution of the approximate level of the 4th floor of the
260 Serapeum is reported in Fig. 6. Also in this figure, as for the Fig. 3, each number refers to a given
261 historical document supporting that level (see Table 2, and Appendix 2). From historical information
262 we know that the 4th floor subsided below the sea level in the 5th century, i.e., about 200 years after
263 its construction during the Severi Age. When the 4th floor reached a level of 3.6 m bsl, around the
264 7th century AD, the columns were wrapped by layers of sedimentary materials, which formed the so-
265 called "fill" (Parascandola, 1947). Then, due to the impact of the relative sea-level change on the
266 coastal area, colonies of lithodomes attached the part of column at the mean sea level, between 3.6
267 and 6.30 water depth (see the two red arrows in Fig. 7c) and created a pitted band above the
268 sedimentary materials, for a thickness of 2.70m. This process occurred until the 9th century AD, when
269 the fourth floor was located to a depth of 6.3 m below sea level. Such a depth was considered by some
270 authors (Parascandola 1947, Amato and Gialanella, 2013) to be the maximum submersion,. In the
271 same period, however, the ground subsidence caused the flooding, by thermal and rain waters, of the
272 Agnano plain, an area located to east of Pozzuoli, and resulted in the formation of a lake (Anecchino,
273 1931). This event indicated a general persistence of subsidence in the Pozzuoli area, which was in
274 fact confirmed very clearly even in the following centuries, as highlighted by numerous historical
275 documents, resumed here (Fig. 7a) and reported in detail in Appendix 2. Such data also contradict the
276 conclusions by Morhange et al. (1999; 2006), who hypothesized a significant uplift, of several meters,
277 in the period 7th-8th century.



279

280 **Fig. 5 – Floors underlying columns of Serapeo (redrawn from Amato and Gialanella, 2013).**
281 **The dotted part of the column indicates the boring due to colonies of *Lithodomus Litophagus*.**
282

283

284 In the 11th century the Arab geographer Idrisi and other historians of 12th century (Benjamin ben
285 Yonah de Tudela) and 13th century (Nicolò Jamsilla), clearly highlighted the morphology of Rione
286 Terra as a medieval castle surrounded by the sea on three sides, due to the continuation of the
287 subsidence, which was still underway at that time (Costa et al., 2022) (see points 6 and 7 in Appendix
288 2). Moreover, in 14th century there is the account of Boccaccio (1355-1373), as reported by
289 Parascandola (1943), who wrote that the fisherman’s wharf in the Bay of Pozzuoli became completely
submerged (point 8 in Table 2 and Appendix 2).

290 We can prove again the subsidence continued further in the following century, since it is possible to
291 get a more precise estimate of the depth below sea level reached by the 4th floor of the Serapeum, by
292 observing the painting “Bagno del Cantariello” (Fig. 7a), part of the famous Balneis Puteolans of the
293 Edinburgh Codex of 1430 AD (Di Bonito and Giamminelli, 1992). The painting depicts the Rione
294 Terra encircled by vertical yellow tuff walls, from which the beach of Marina Della Postierla extends
295 (towards the observer) to the base of the S. Francesco hill, the source of the thermal spring Cantariello
296 (foreground) near the coast northeast of the submerged Serapeum. Behind the visitors of the thermal
297 spring, the painting clearly shows the upper part of the three marble columns of Serapeum emerging
298 from the sea. Also depicted are people fishing directly from the shore (Fig. 7b). From this painting

we can make a rough estimate of the portion of columns below the sea level at that time, taking into account that a significant part of the columns is submerged. Historical records from the 1750 excavations, (see further) indicate that the buried part of the columns amounted to about 10 m (see Parascandola, 1947); the shallowest 2 meters of the excavations were formed by pyroclastic flow deposits of the 1538 eruption (see further paragraphs).

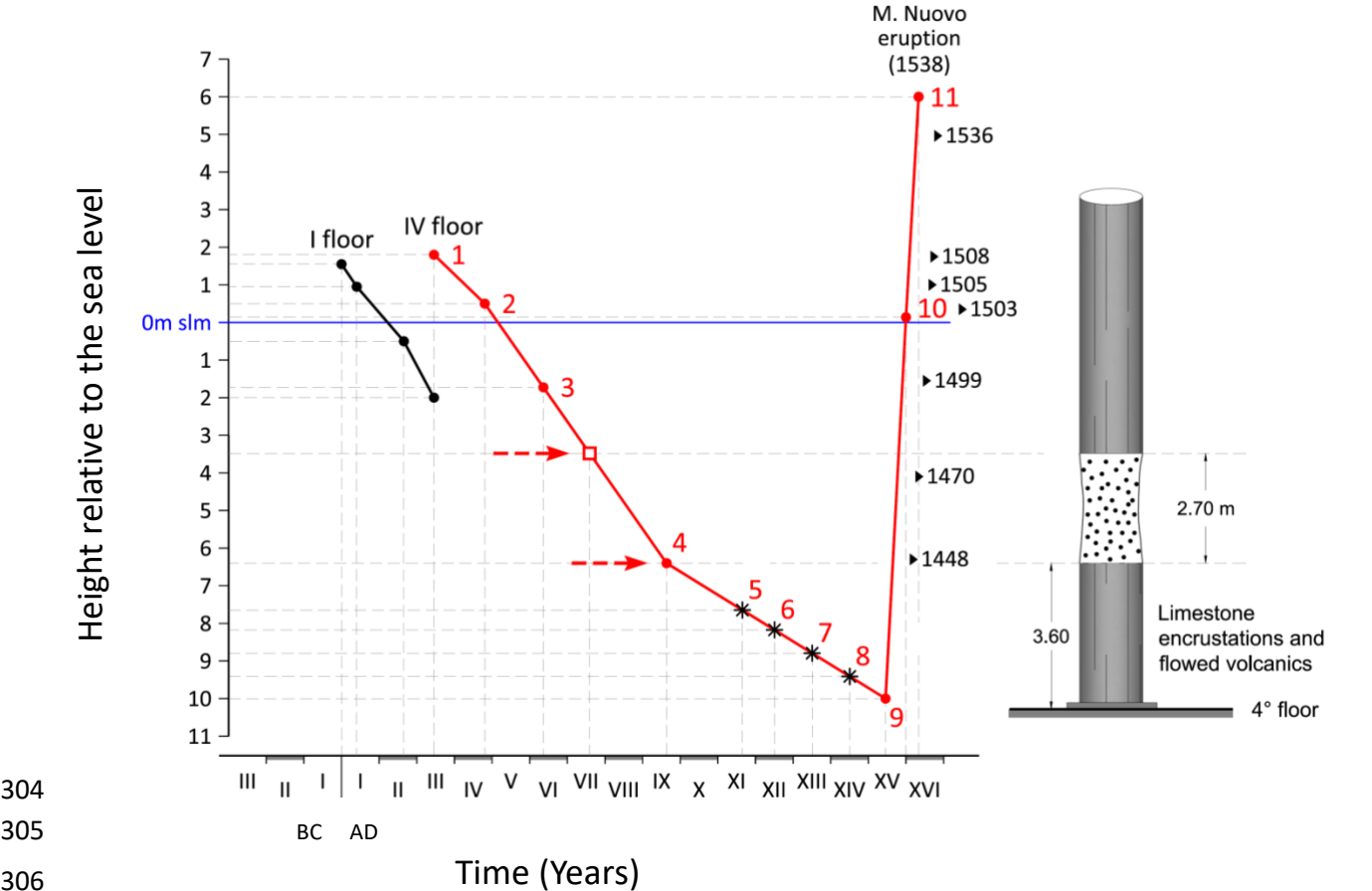


Fig. 6 – Diagram of the level of first (until the building of the fourth floor) and fourth floor of the Serapeum The arrows indicate the limits of the submersion corresponding to the part of the columns bored by lithodomes. Numbers on the curve indicate the times of references for the inferred level: they are synthetically reported in Table 2 and extensively explained in the Appendix 2. Dates marked on the right indicate the times of occurrence of major earthquakes.

Number	Time	Event	Reference source
1	230 AD	The third floor of Serapeum was at a level of only about 1 m asl, often invaded by water: it was then built the fourth floor, located at 2 m asl	Amato and Gialanella, 2013
2	394 AD	The fourth floor is invaded by the sea. Important works to	Camodeca, 1987; Caruso, 2004

		restore the banks and protect them by coastal embankments	
3	VI-VII century	Puteoli almost depopulated. People refuged in a fortified citadel, surrounded by sea: the Acropolis of Rione Terra	Varriale, 2004
4	VIII-X century	Due to continuous subsidence, Agnano Plain was invaded by water, transforming into a lake	Annechino, 1931
5	XI century	The sea increasingly surrounded Rione Terra, which appeared like a castle. The Arab geographer <i>Idrisi</i> in his <i>Opus Geographicum</i> , describing Pozzuoli as a "castle"	Varriale, 2004
6	XII century	Subsidence continues: Benjamin ben Yonah de Tudela, passing through Pozzuoli, described: <i>turres et fora in aqua demersa quae in media quondam fuerant</i>	Russo Mailer C., 1979; Caruso, 2004
7	XIII century	Subsidence continues: Niccolò Jamsilla (<i>Historia de rebus gestis Frederici II imperatoris ejusque filorum Corradet Manfredi Apuliae et Siciliae regnum</i>) describes the places between Agnano and Pozzuoli as follows: <i>...videlicet Putheolum mari mantibusque inaccessibilius circumquaque conclusum...</i>	Fuiano, 1951
8	1327-1341	Boccaccio reported descriptions as the lower part of Puteoli being completely submerged	Mancusi, 1987
9	1430	The 1430 gouache 'Bagno del	Di Bonito and Giamminelli, 1992

		Cantariello' shows the Serapeum columns submerged for about 10 meters. A	
10	1441	A description indicates that 'the sea covered the littoral plain, today called Starza'	De Jorio, 1820

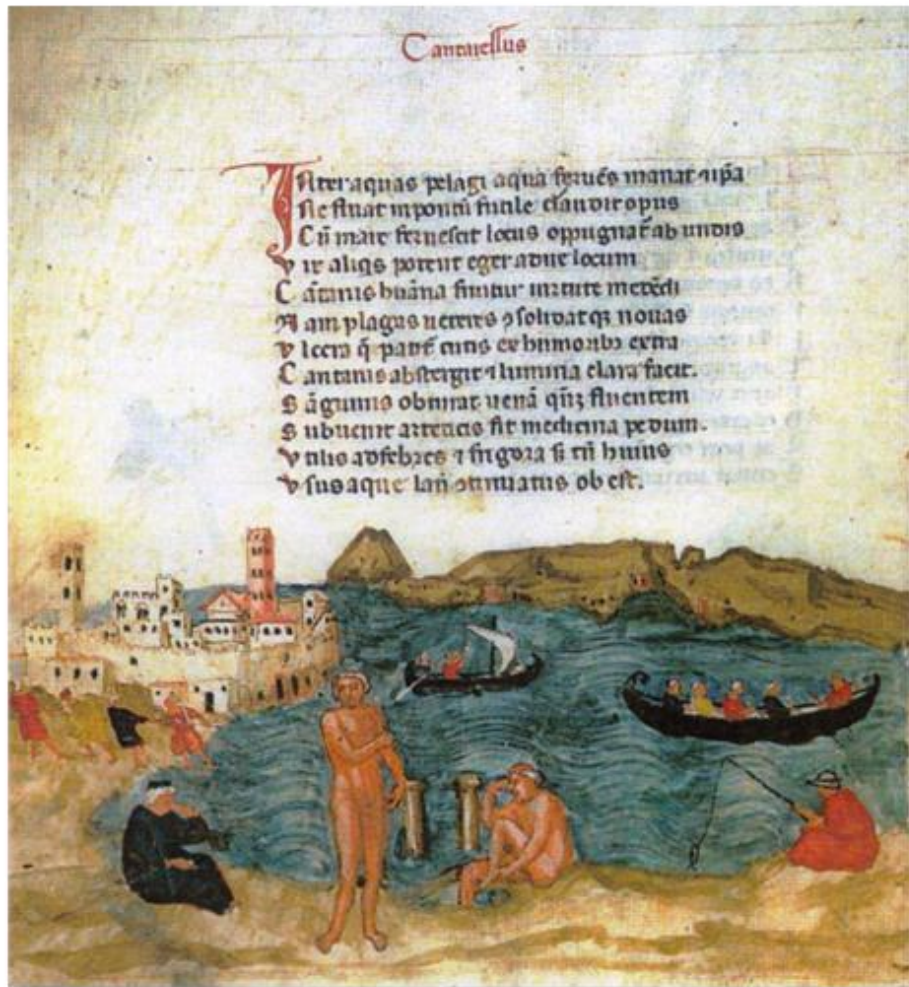
313

314 **Table 2: Synthetic sketch of the main historical sources used to reconstruct the ground**
315 **deformations shown in Fig.6 (see Historical Appendix 2 for more details).**

316

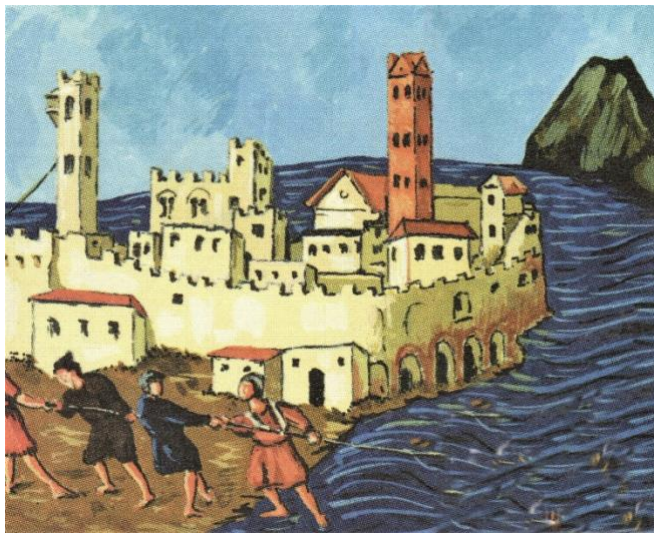
317 This observation constitutes an indication that during the time of the painting (1430), in the absence
318 of 1538 products, the buried part of the columns should then have been approximately 8 meters.
319 Moreover, the presence of trawling fishermen in the scene (Fig. 7b) suggests that sea depth there did
320 not exceed 2 m (the maximum water depth for this type of fishing not far from the beach). Given that
321 the total height of the columns is 12.7 m, we estimate that the emerged part of the column in 1430
322 was around 2.0-3.0 m (Fig. 7a,c).

323

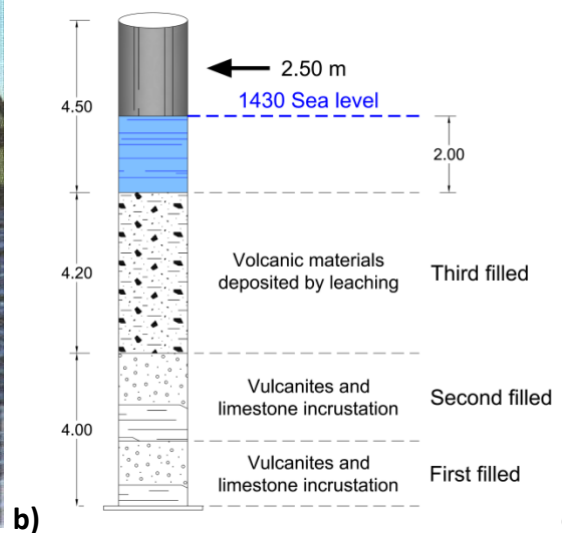


324

a)



325



b)

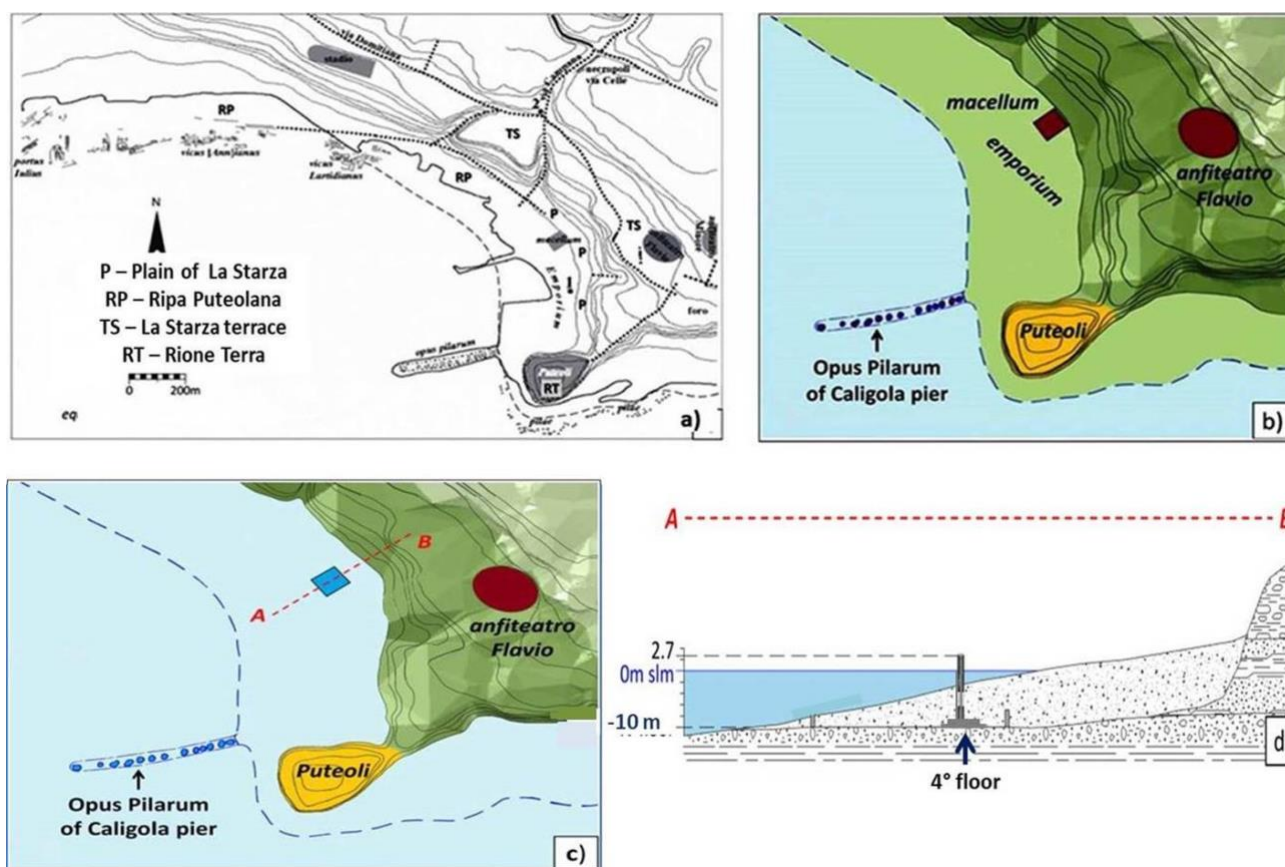
c)

326

327 Fig. 7 – Gouache of de' Balneis Puteolanum from 1430: a) Stumps of the Serapeum columns
328 that protrude from the sea to a height of 2-3m, b) Fishing from the shore, highlighted in the

329 box, indicates a draft depth of approximately 2m of sea, c) Reconstruction of the submerged,
 330 emerging and buried parts of the columns (see text for complete explanation).

331



332

333 Consequently, we infer that in 1430 AD the floor was about 10 m (+/-1 m) below sea level (Fig. 6).
 334 Such deduction, derived from the context represented in Fig.7a, can be explained in even greater
 335 detail with the help of the topographic map of the Pozzuoli area in Roman times (Soricelli, 2007)
 336 (Fig. 8a).

337

338 **Fig. 8 – a) Map of Pozzuoli from the Roman era (III-IV century).** The map shows the lower part
 339 of the emporium which extends along the Puteolana bank (RP), until reaching the base of the
 340 hill, the so-called Starza plain (P) and the upper part of the Rione Terra cliff (RT) which, in
 341 turn, connects with the upper hilly part of the Starza terrace area (TS). b) Part of the previous
 342 map, limited to the Emporium Area, in the Middle Age (after Aucelli et al., 2020, and Taravera,
 343 2021). c) the same area shown in b around 1430, during which the hill areas (TS, RT) were
 344 surrounded at the base by the sea, according to a description of the lower area of Pozzuoli from
 345 1441 "the sea covered the littoral plain, today called Starza" (after De Jorio, 1820; Dvorak and
 346 Mastrolorenzo, 1991). d) sketch of the profile A-B shown in c: the sea extended behind the

347 **Serapeum on the plain of La Starza hill, intersecting the columns at a height of 10m (also**
348 **shown).**

349

350

351 The map (contour lines of 5m), shows that in the period of greatest development the city included the
352 Greek Acropolis (the ancient Dicearchia nowadays called Rione Terra), with a maximum height of
353 40 m asl, the lower part of the city, i.e. the western area overlooking the ancient emporium and the
354 Serapeum (Roman macellum) placed near the bay area, and the upper city on the Starza terrace, with
355 elevation between 30-50 m asl. The latter was the site of the ancient monumental edifices
356 (amphitheatre, stadium, forum, necropolis, etc.). From this map, considering only the area of the
357 Emporium (lower part) and amphitheater (upper part), a sketch of topographical relief above the sea
358 level (in Roman times, Fig. 8b) and underlying sea level (in 1430 AD, Fig. 8c) has been obtained and
359 described as follows:

360 - from profile A-B of Fig. 8c, as reported in Fig. 8d, the 4th floor of the Serapeum can be located at
361 a depth of 10m, packed in the sediments that form the Ripa Puteolana (RP), with the columns
362 protruding from the same sediments for 4.5m, of which approximately 2m are sea water. It is
363 indicated, ultimately, that the sea level intersects the columns of the Serapeum at a height of
364 approximately 10 m, connecting with the contour line of 10 m, on the La Starza Plain (P) (Fig. 8c,d).
365 - Fig. 8c also allows us to highlight the morphological conditions of the Rione Terra, which, as we
366 have already observed, has been described by the chroniclers who visited this place from the 11th to
367 the 13th century as "*an unapproachable mountain completely surrounded by the sea*" (Fuiano, 1951;
368 Varriale, 2004, in Appendix 2).

369 The historical data presented here highlight an evolution of the ground movements in the area very
370 different from hypotheses appeared in previous literature. They mainly confute results published in
371 the most recent work on such an argument (Di Vito et al 2016), who made the following claims:

- 372 1) the subsidence in the area started in 35 BC;
373 2) the local uplift in the area of the 1538 vent, from 1536 to 1538, amounted to about 19 m.;
374 3) the maximum subsidence was reached in 1251.

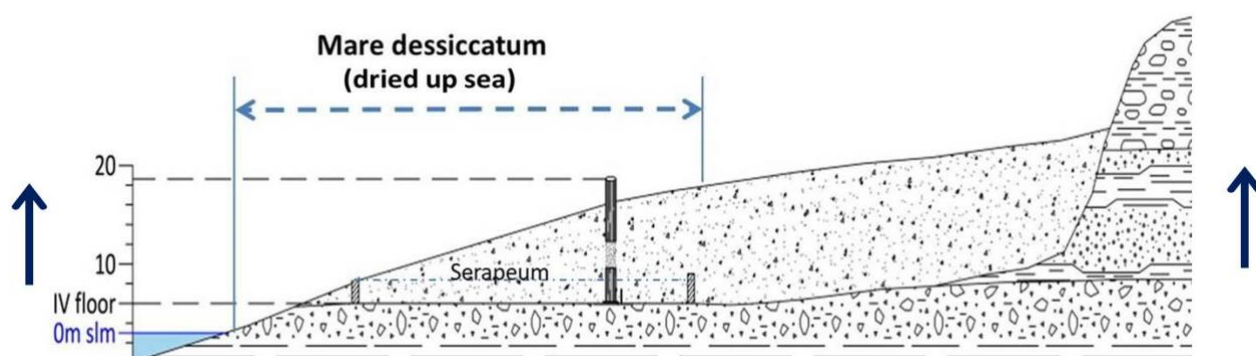
375 The first claim is in contrast with at least two strong evidences, coming from historical documents:
376 that already at the times of Greek colonization (end of 8th century BC) the Via Herculea used by
377 Greeks, showed signs of subsidence (see Diodoro Siculo in Appendix 1) (Fig. 2); limiting ourselves
378 to the documents of 1st century BC, it is sufficient to observe that, due to the subsidence of this dam,
379 Giulio Cesare himself was sent by the Roman Senate in 48 BC, to fix the problem, which was resolved

380 more constructively by Agrippa in 37 BC, raising the surface of the Via Herculea with respect to the
 381 sea level (see again detailed explanation in Appendix 1).

382 Claim 2) can be easily demonstrated to be not realistic, because in case of uplift in the Monte Nuovo
 383 area higher than few meters, the Via Herculea would have risen back above the sea level (Fig.3d).

384 Claim 3), finally, is not confirmed by the testimonies collected until 1430, which instead indicate the
 385 continuation of this phenomenon (Di Bonito and Giamminelli, 1992; Bellucci et al., 2006).

386



387

388 **Fig. 9 – The uprise of the land (marked by the two arrows on the sides) was observed and**
 389 **described by Loffredo Ferrante in 1530: "the sea was very close to the plain which was at the foot**
 390 **of the Starza hill". In this context, the 4th floor of the Serapeum had reached a height of**
 391 **approximately 4 m above sea level.**

392

393 From our reconstruction, based on reliable historical documentation, we demonstrate that the
 394 hypothesis that maximum submergence depth of the 4th floor of the Serapeum was reached in the 9-
 395 10th century, proposed by Parascandola (1947) and Amato and Gialanella (2013), is not realistic. Nor
 396 it is the hypothesis by Di Vito et al. (2016), who place the date of the transition between subsidence
 397 and uplift in the 13th century and precisely in 1251.

398 Our findings, dating the starting phase of uplift around 1430, are also supported by the documented
 399 occurrence of the first documented powerful earthquake in 1448 (Colletta, 1988: see also next
 400 paragraph), which induced King Ferdinand I of Aragon to suspend the so-called "fuocatico" (a
 401 mediaeval tax collected for each fire lit by a family unit; see Colletta, 1988). We know in fact, from
 402 recent unrests, that earthquakes only occur during the uplift phases at Campi Flegrei (Troise et al.,
 403 2019). It is also well known that, between 1503 and 1511, the municipality of Pozzuoli granted the
 404 lands that emerged, as a result of the increasingly "drying up sea" (Fig. 9), expanding the available
 405 land, to citizens requesting them (Parascandola, 1947). Bellucci et al. (2006) and Dvorak and
 406 Mastrolorenzo (1991), however, also reported a date around 1430 or later for the beginning of the
 407 uplift phase; so, the data presented here (partly already used by Bellucci et al., 2006 and Troise et al.,

408 2007), support their interpretation, although making it more precise and robust by the addition of new
409 data.

410 The next important question is then: was the 4th floor of the Serapeum above sea level as early as at
411 the beginning of 16th century? Parascandola (1947) answered this question through a sentence found
412 in an account by Loffredo Ferrante from 1580: *In 1503 the sea was very close to the plain which was*
413 *at the foot of the Starza hill* (Fig. 8). So, it can be deduced that the floor of the Serapeum in the 1503
414 was just above sea level, that is, it had risen about 10m in about 73 years, with a rate of 136 mm/y.
415 There is clear evidence that the uplift phase continued until 1538, when the eruption occurred. The
416 maximum uplift occurred in the Pozzuoli area, close to the Rione Terra cliff, that up to the 1538
417 eruption reached an elevation in the order of 5-6 m asl (Fig. 6).

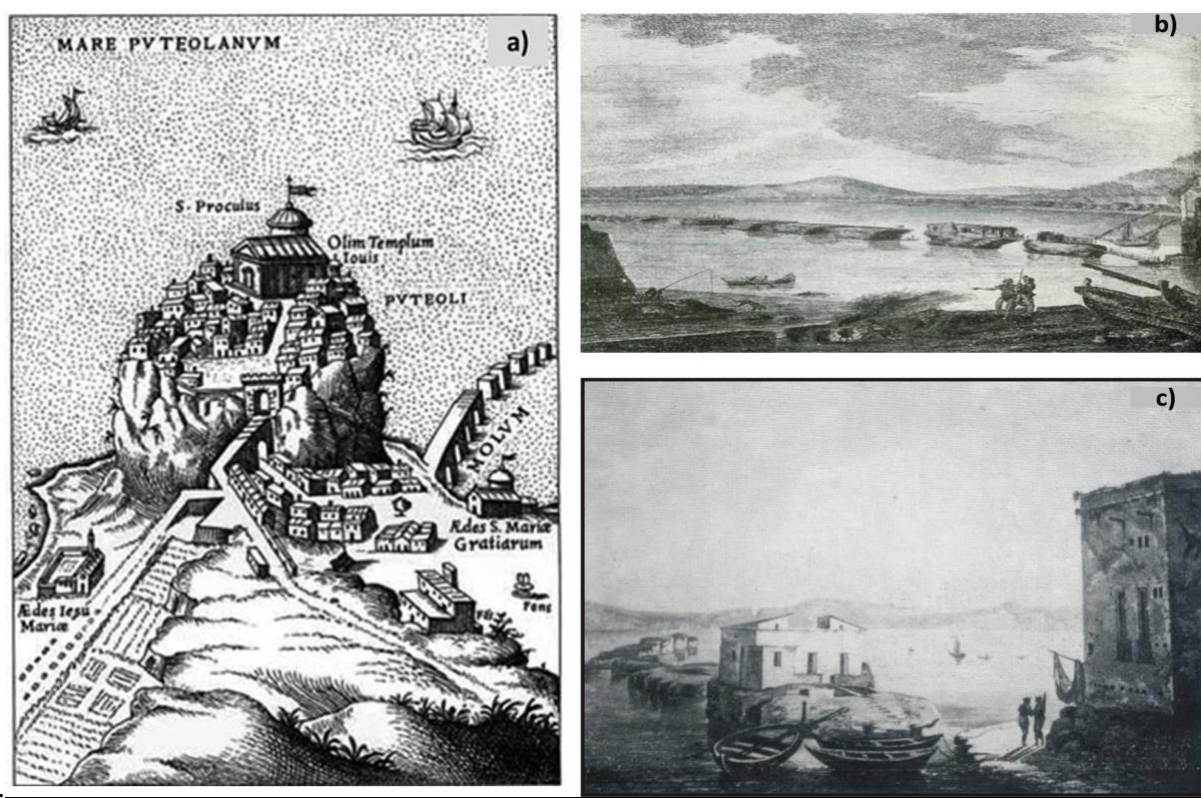
418 In the nearby area facing Averno to the west, the uplift, as already said, was unable to cause emersion
419 of the Via Herculea. So, the vent area could be affected by an additional uplift, occurred just before
420 the eruption, however such that the total uplift since 1430 resulted lower than about 7m. In the eastern
421 sector of the caldera, at Nisida island, the pier did not emerge above sea level (Parascandola 1947).
422 It is then very likely that the uplift phase had a bell-shaped trend, very similar to what we see in the
423 recent unrests, except for a marked additional uplift at the vent site, just before the eruption
424 (Parascandola, 1943), however limited to a total of about 7 m maximum, possibly due to upward
425 migration of the dyke feeding the eruption.

426

427 1. Ground movements after the 1538 eruption

428 The period between the end of the 16th century and the beginning of the 17th century lacks any written
429 historical document testifying the ground movements at Pozzuoli. It is likely that after the 1538
430 eruption a subsidence phase started, probably after the last, post-eruption, seismic phase ended in 1580,
431 as it will be shown in the following paragraphs. We can anyway learn something from some paintings,
432 the oldest one by Cartaro, dated 1584 (Fig. 10a), which highlights the Rione Terra in the foreground,

433 with the Neronian pier which emerges almost completely above sea level, which means for about 5-6



434 m.
435 **Fig. 10 – a) Engraving by Cartaro (1584) showing the Neronian pier at the base of the Rione**
436 **Terra, emerging from the sea for 5-6m, showing 10 of the 15 piles of which it was made up in**
437 **roman epoch, b) The remains of the pier piles, without the upper arches, highlighted in an**
438 **engraving from the mid-18th century, c) Detail of the same piles highlighted in another**
439 **engraving from the same period, where the height of the 1-2m piles is observed in more detail,**
440 **subject to marked erosion**

441
442 It also appears still partially complete, with about half pylons still connected with arches (*Opus*
443 *Pilarum*). In comparison, paintings from the middle XVIII century (Fig. 10b,c) report the pier
444 completely destroyed, and clearly almost completely submerged; the painting of Fig. 10c represents
445 the pylons in more detail, allowing to estimate the height of the emerging part asl around 1-2 m. Fig.
446 11 shows another famous painting of 1776, by Hamilton, which shows the ruins of the Neronian pier
447 almost the same way than in Fig. 10b,c and, in addition, shows the columns of Serapis Temple, with
448 its floor almost at the same level than the Neronian pier.

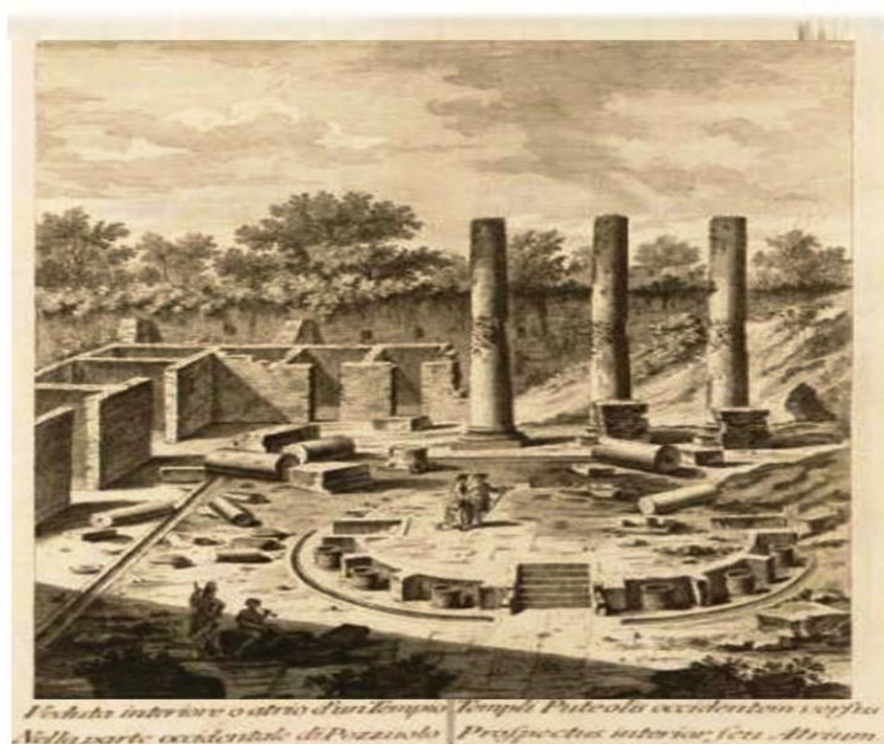
449



450

451 **Fig. 11 – a) View of the Gulf of Pozzuoli and the Cape Miseno peninsula (Hamilton 1776).**
 452 **Both the remains of the Neronian pier and the newly excavated Serapeo are also visible**

453



454

455 **Fig. 12 – Illustration of Serapeum, as excavated in the three-year period 1750-1753. It can be**
 456 **noted that the height of the lighter parts of the columns, including the pitted band of the**
 457 **lithodomes, is preserved by oxidation, because packed by the just removed sediments. The**
 458 **darker upper part, oxidized since staying outside the cover, has a height of approximately**
 459 **2.50m, estimated on the same figure. This leads us to consider that the pack of sediments**
 460 **removed had a thickness of approximately 10m, that is, the height of the hill where the vineyard**
 461 **of the three columns was located before the excavation (Niccolini, 1842).**

462

463 From the comparison of Fig. 10a with 10b and 10c it can be deduced that the Roman opus pilarum
464 underwent a subsidence of about 4-5 m. from 1580 to 1750.

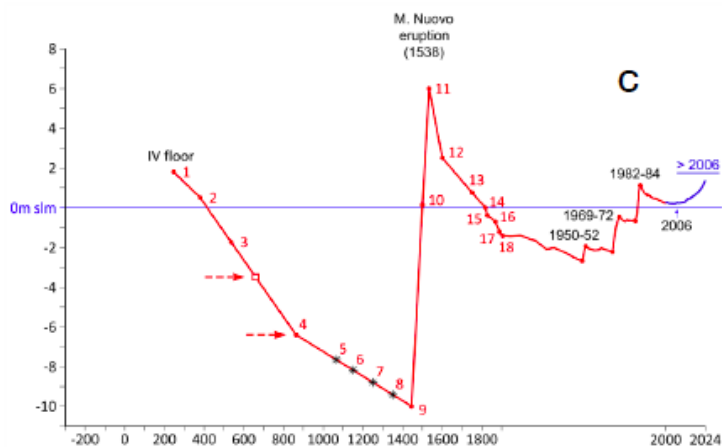
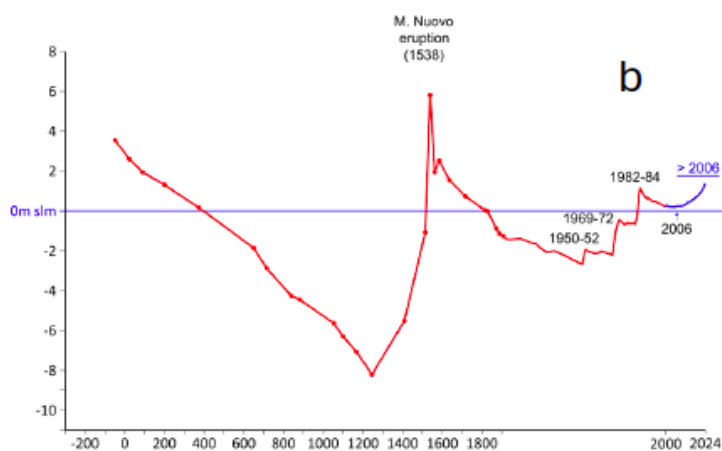
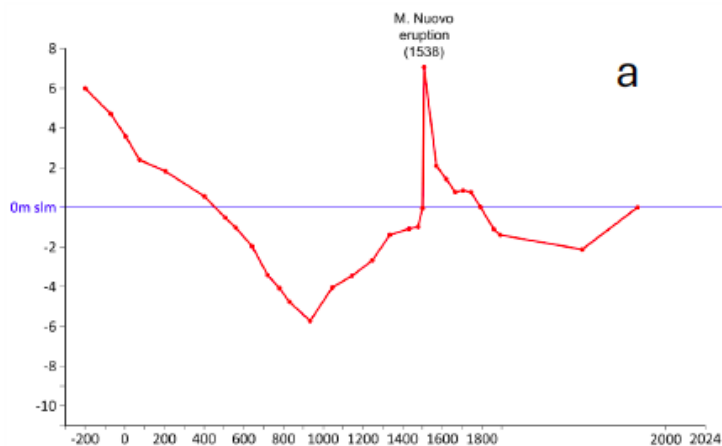
465 Since the floor of the Serapis Temple appears to be at the same level than the pier, its level in 1538
466 can be estimated as 5 – 6 m. above sea level (Fig. 6), while in 1750 it should be at about 1m above sea
467 level, with an estimated subsidence 1580-1750 of about 4-5 m. This approximate estimation is however
468 confirmed by Parascandola (1947), who reports some measurements by Niccolini (1846), who found
469 the 4th floor of Serapeo to have a height above sea level varying in the range 0.9 - 0.6m throughout
470 the 18th century. It can then be deduced that during the three years of the excavations (Fig. 12) the
471 floor could have been approximately at 0.7 m above sea level.

472 Finally, we want to highlight, in agreement with Parascandola (1947), that the subsidence of 4 - 5 m,
473 started after 1580, could have evolved at higher initial rate, in such a way that, around the middle of
474 the 17th century, it already had a value of 2 -3 m, and then slowed down towards the end of the
475 century, until the 1750.

476 It is also interesting to compare the average subsidence rate before 1430 with that observed after 1538
477 till 1950. The overall rate of subsidence after 1538 is about 2 cm/year, almost double with respect to
478 that observed before 1430. However, when excluding the first phase of sharp subsidence occurred
479 just after the 1538 eruption, the subsidence rate becomes very similar to that observed since the roman
480 era until 1430.

481 We are hence able to describe in more detail the whole evolution of ground movements at the Pozzuoli
482 area since Roman times, including the period following the 1538 eruption and until today. Such a
483 reconstruction is shown in Fig. 13c. In particular, regarding the post-1538 subsidence phase, the data
484 shown, starting from the 17th century, have been combined with those obtained by the most
485 significant measurements carried out by numerous researchers who dealt with this phenomenon
486 during the 1800s, as reported by Parascandola (1947), who suggested the reconstruction shown in
487 Fig. 13a. High precision, frequent measurements started to be collected since 1905, initially based on
488 leveling surveys carried out by the Military Geographic Institute (IGM). Data from the levelling
489 surveys were still provided also during the occurrence of the most recent unrest phases, i.e. in 1950 -
490 52, 1969 – 72, 1982 – 84 and until 2001. Since 2001, continuous measurements are provided by GPS
491 (RITE, see Fig. 13b,c) installed at Rione Terra (Del Gaudio et al 2010).

Height relative to the sea level



Time (Years AC)

Fig. 13 a) Reconstruction of the ground level of the Serapeum floor, with respect to the mean sea level (blue line), as proposed by Parascandola (1947); b) Reconstruction of the Serapeum floor ground level, recently proposed by Di Vito et al. (2016); c) Reconstruction of the ground level of the Serapeum IV floor, since III century A.D. to present, inferred by this study. Each

point in the diagram corresponds to an appropriate historical indication reported in Table 1 and in the Appendix 2.

2. Schematic model for the preparatory phases of the 1538 eruption

2.1 Dynamics of the resurgent block in response to temperature and pressure perturbations

The ground deformation at Campi Flegrei, during the phases preceding and following the 1538 eruption, has been likely very concentrated in a small area of few km of radius around Pozzuoli, just as during the recent unrests (De Natale et al., 2001; 2006; 2019). Such a concentration agrees with the presence of a resurgent block.

Evidence for the involvement in the Campi Flegrei unrest episodes of a resurgent block comes from the first observations and modeling by De Natale and Pingue (1993). These authors pointed out that the concentration of the uplift in a small area, the high uplift values, and the invariance of the uplift and subsidence shape, as well as of the seismic area, indicated the up and down movement of a resurgent block, bordered by ring faults focusing the occurrence of earthquakes (see also De Natale et al., 1997; Beauducel et al., 2004; Troise et al., 2003; Folch and Gottsmann, 2006). Some authors proposed that ground deformations could be explained also without any effect of bordering faults (Berrino et al., 1984; Bianchi et al., 1987; Amoroso et al., 2008, 2014; Woo & Kilburn, 2010); however, most of these models required some ‘ad hoc’ distribution of rock rigidity, sometimes not realistic (see De Natale et al., 1991), or required an unrealistic constancy of the source geometry able to explain the remarkable constancy, during several decades or centuries, of the shape of deformation during both uplift and subsidence (see De Natale et al., 2006). All of these models, in addition, do not explain the peculiar shape of the seismic area, being almost elliptical around the most uplifted area. In recent times, new evidence has been collected about the location and limits of the resurgent block (Rolandi et al. 2020b). Furthermore, active high-resolution reflection seismic surveys have pointed out and imaged the presence, in the Gulf of Pozzuoli, of an inner resurgent antiformal structure or “block” bounded by a 1-2 km wide inward-dipping ring fault system associated with the caldera border, whose limits have been also documented by the survey (Sacchi et al., 2014 Steinmann et al, 2016; Sacchi et al., 2020a). Further constraints for the extent on-land of the resurgent block come from stratigraphic evidence. In particular, the old well CF-23, drilled in the Agnano area, presents about 900 m of NYT deposits, topped by only 100 m of more recent deposits (Rolandi et al. 2020b). The presence of uplifted, thick layers of NYT, characterizes the stratigraphy of all the wells contained in the resurgent block (Fig.14a,b,e), thus allowing to map its extent on-land, although only the CF-

23, by far the deepest one, clarifies the whole thickness of the NYT deposits in the resurgent area (Fig. 14a,c,d).

The extent of the resurgent block on-land appears also reasonably well defined by a clear relative gravimetric maximum (Capuano et al., 2013). It is crucial to emphasize that the differential movement of the resurgent block, mostly detached from the external caldera rocks, is responsible for the almost constant, highly concentrated shape of ground displacement, during both uplift and subsidence. The resurgent structure is also associated with distinct seismicity along the bordering ring fault zone (see also Troise et al., 2003). Fig. 15a-c shows how the resurgent block is well evidenced by passive seismic data (Fig. 15b, c) and by earthquake locations (Fig. 15a).

The presence of the central, resurgent block significantly affects the dynamical behavior in response to temperature and pressure perturbations. This is particularly evident in the central, most deformed and seismic area, where the shallow crust involves approximately 1.5 km of lithoid tuff. This contradicts substructure models proposed by various authors (Rosi and Sbrana, 1987; Vanorio et al., 2002; Lima et al., 2021; Kilburn et al., 2023), which often assume a thick shallow layer of loose pyroclastics from recent eruptions, typically represented by the stratigraphy of well SV1 (see Fig. 14e).

The physical state of the shallow structure within the resurgent block can be inferred by seismic tomography analyses presented by several authors (e.g. Aster and Mayer, 1998; Vanorio et al., 2005; Vinciguerra et al., 2006; Battaglia et al., 2008; Calò and Tramelli, 2018). These analyses consistently indicate a high V_p/V_s ratio centered below Pozzuoli town down to 1-2 km, interpreted as highly water saturated tuff.

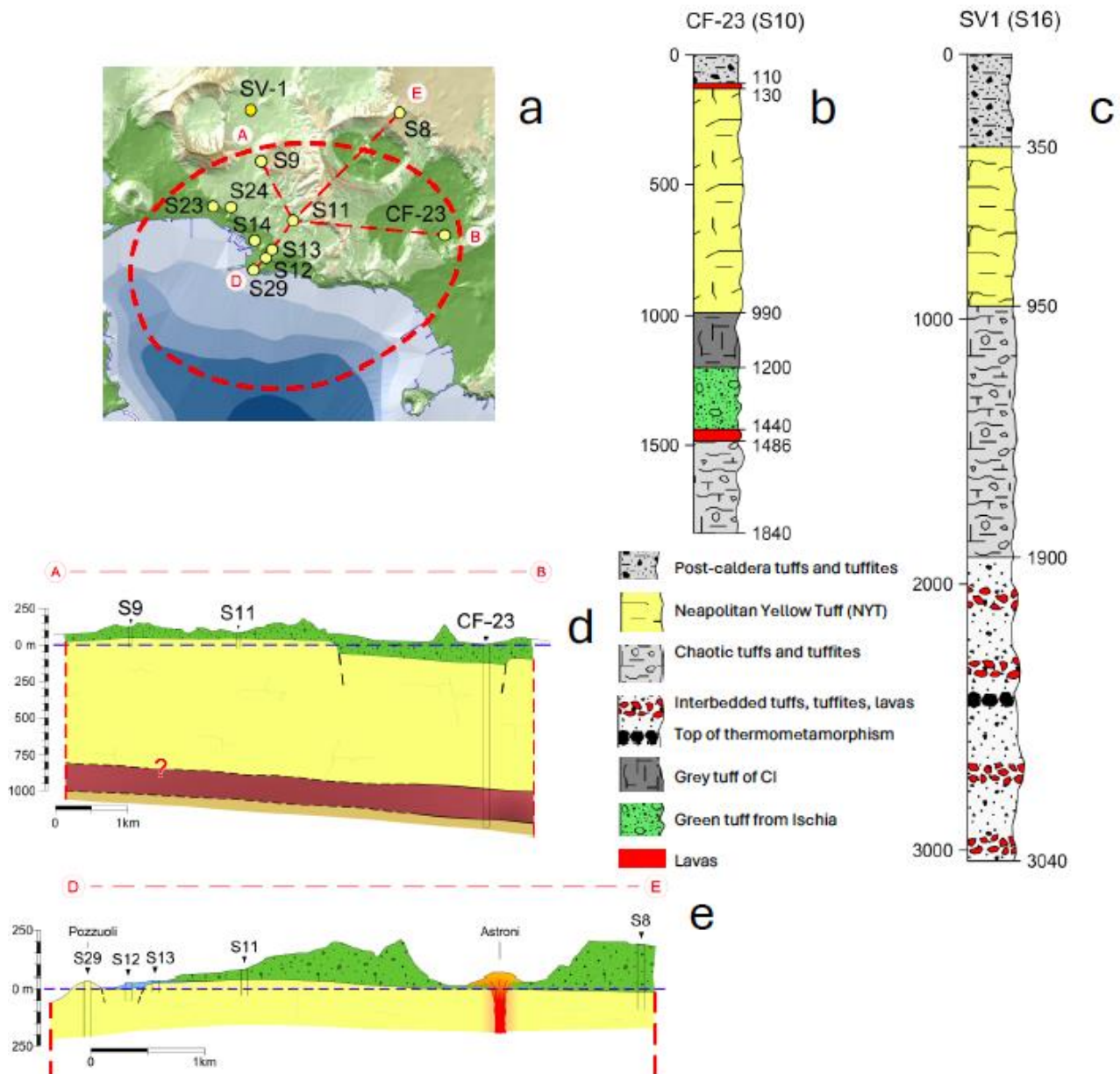
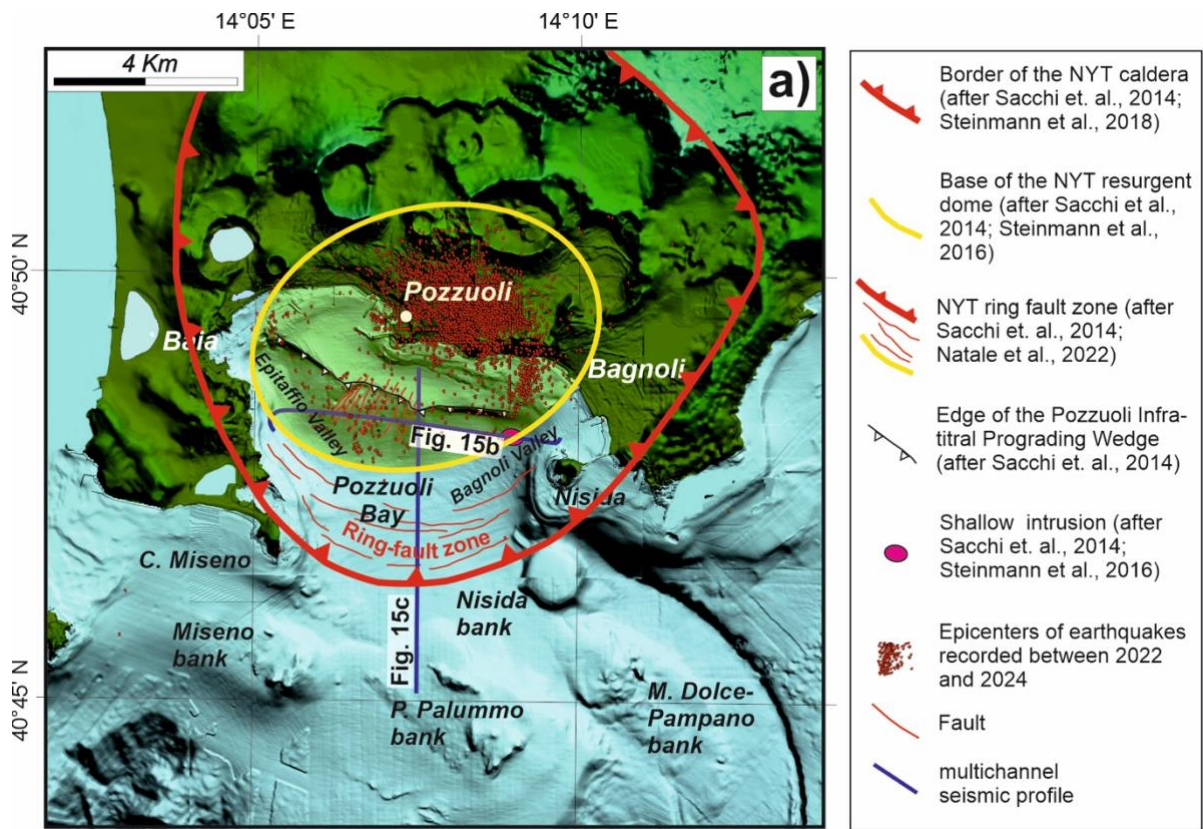


Fig. 14 - a) Location of the wells explored within the resurgent tuff block, as reported in literature; b) Stratigraphy of the CF23 (S10) well, within the resurgent block; c) Stratigraphy of the SV-1 well, outside the resurgent block, which highlights a stratigraphy where the NYT tuff blocks are not present with significant thicknesses; d-e) Profiles in the resurgent block which highlight the shallow depth of NYT because of the resurgence.

Of particular significance is the work by Vinciguerra et al. (2006) which compared the results of seismic tomography with laboratory tests. They demonstrated that the tuffs present in the central area of the Campi Flegrei caldera can be either water or gas saturated, and that inelastic pore collapse and cracking produced by mechanical and thermal stress can significantly alter the velocity properties of Campi Flegrei tuffs at depth. The effect on velocities becomes significant when the temperature rises

566 sufficiently to induce physical changes, such as volume change and the generation of free water
 567 associated with the dehydration of zeolite phases. This can lead to thermal crack damage (see also
 568 Chiodini et al., 2015; Moretti et al., 2018), further affecting the dynamic behavior of the area. At
 569 higher depths, the well CF-23 indicates the presence of pyroclastic deposits from a depth of
 570 approximately 1.5 km to at least 1.8 km, where a temperature of 300°C was measured (Fig. 14b).
 571 Likely, at even greater depths of about 3km, marine silt and clay layers induce silica mineralization
 572 and the formation of low-permeability horizons. Due to the high temperatures, estimated to be at least
 573 400°C, these layers undergo thermal alteration, forming a thermo-metamorphosed layer (Fournier,
 574 1999; Lima et al., 2021; Cannatelli et al., 2020).
 575 Is important to note that Battaglia et al. (2008) interpreted a low Vp/Vs body, extending to about 3–
 576 4 km of depth, as due to the presence of fractured overpressured gas-bearing formations, confirming
 577 the data of Vanorio et al. (2005). This depth range of 3-4 km likely represents a primary accumulation
 578 zone
 579

580



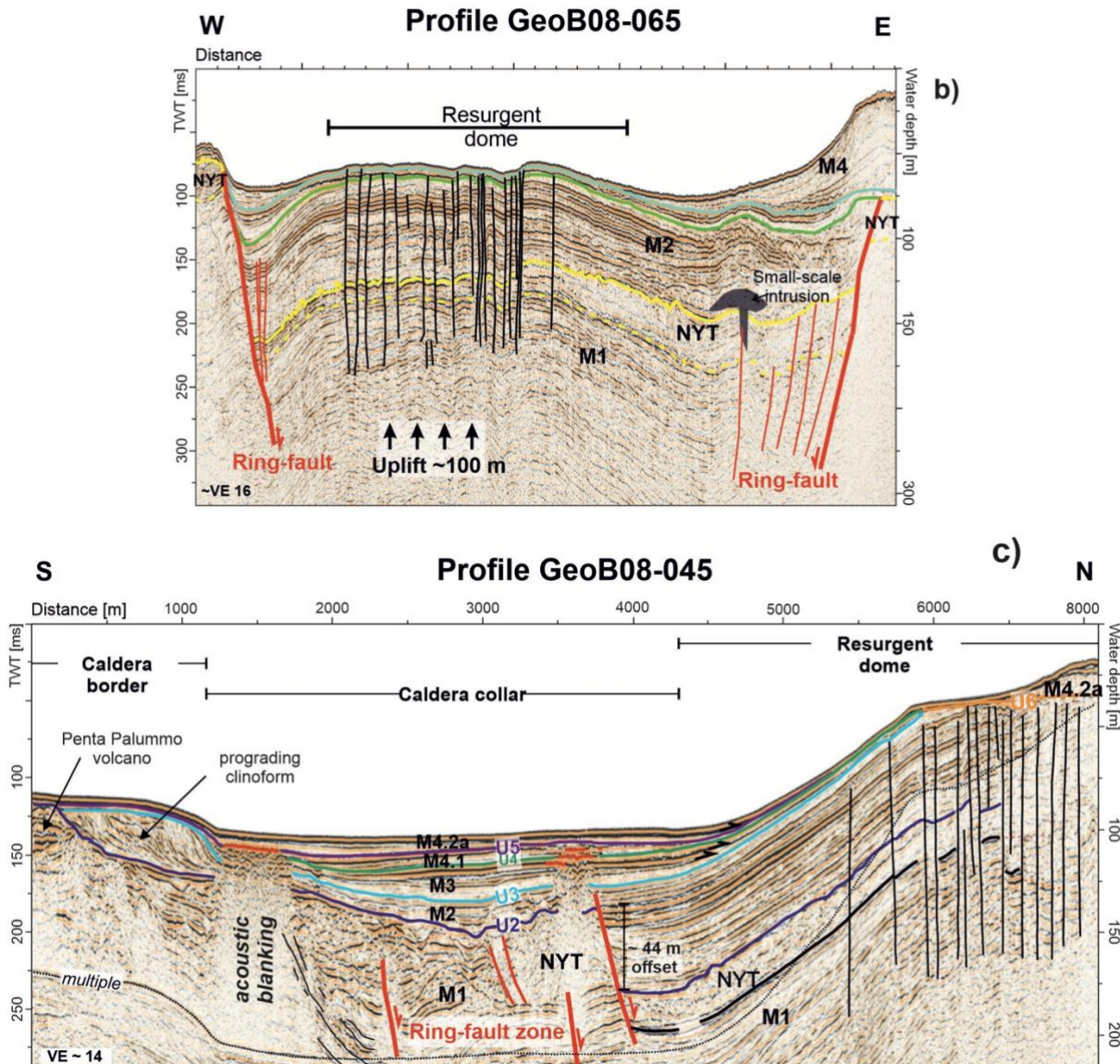


Fig. 15 – a) Campi Flegrei map showing the approximate limits of the resurgent block (area in the yellow ellipse), which concentrates ground deformation and seismicity. b) The N-S and c) W-E profiles of the high-resolution seismic survey, showing the offshore signature of the NYT ring fault system and resurgent structure (from Sacchi et al., 2014, 2020a, 2020b; Steinmann et al., 2016).

for shallow intruded magma, which is unable to reach the surface and instead forms magma sills (Woo and Kilburn, 2010; Di Vito et al., 2016; Troise et al., 2019; Kilburn et al., 2023). The magma at this depth is likely to be in a mush state, i.e. solidified but still at temperature high enough to be remobilized by the inflow of new magma or hot magmatic fluids (De Natale et al., 2004). At even greater depths, approximately between 7 - 8 km, the main magma chamber is located. This chamber contains both liquid magma and residual mush from past eruptions (Judenherc and Zollo, 2004).

595

596 **5.2 The preparatory phases of the 1538 eruption**

597 A tentative model can be now constructed for the preparatory phases of the 1538 eruption, which
598 accounts for all available data. It is shown in Fig. 16, and can be summarized as follows:
599 the Pozzuoli area experienced a long period of subsidence, beginning at the end of the second phase
600 of post-caldera volcanism (3.7 ka B.P.) and lasting until 1430 AD. This subsidence was likely triggered
601 by the collapse of the upper and middle crustal blocks into the underlying magma chamber, situated
602 deep within the limestone basement at depths of 7-8 km (Judenherc and Zollo, 2004). The viscoelastic
603 behavior of the shell encasing the magma chamber may have also contributed to the subsidence, along
604 with the decrease in magma volume due to cooling and crystallization (Fig. 16a).
605 Since the end of the second phase of post-caldera volcanism, approximately 3.7 ky ago, the primary
606 magma chamber, located at 7-8 km of depth, likely contains a mixture of liquid magma and mush. It's
607 important to note that mush refers to a non-eruptible phase of trachytic magma, composed of 25%–
608 55% volume by crystals (Marsh, 1996; Bachmann and Huber, 2016; Cashman et al., 2017; Edmonds
609 et al., 2019). When heated by several tens of degrees, typically through the injection of hotter magma,
610 mush can revert to a liquid state, thereby regaining the ability to trigger a volcanic eruption (e.g. De
611 Natale et al., 2004; Caricchi et al., 2014). However, the way the mush is rejuvenated by intrusion plays
612 a fundamental role in this mechanism (Parmigiani et al., 2014). One plausible scenario is that the new
613 magma from the deeper crustal levels forms sills at the base of the mush, revitalizing it through the
614 supply of heat, but not of magmatic mass, i.e. only exsolution occurs (Bachmann and Bergantz, 2006;
615 Bergantz, 1989; Burgisser and Bergantz, 2011; Huber et al., 2011; Bachmann and Huber, 2016;
616 Cashman et al., 2017; Carrara et al., 2020). To explain the rapid uplift observed in the interval between
617 1430 and 1538, the temperature contrast between the two layers could play a fundamental role: the
618 mafic melt positioned at the base, being hotter than the overlaying layer, undergoes cooling and
619 crystallization, leading to an increase in the volatile content (primarily H₂O and CO₂) of the residual
620 melt (Fig. 16b). Lower ductile rocks tend to deform gradually, allowing magmatic gases to permeate
621 into the brittle zone above, thereby inducing a thermo-metamorphic separation layer.
622 A seismic anomaly displaying low V_p/V_s at approximately 4 km depth (Battaglia et al., 2008)
623 indicates the presence of supercritical fluids. Earthquakes are clustered above such a depth,
624 suggesting the presence of fractured rocks rich in overpressured gas. This condition likely results in
625 triggering additional earthquakes (Fig. 16a): a similar condition has been often hypothesized to occur
626 in the Yellowstone volcano (Shelly and Hurwitz, 2022), and is explained in the following. Intense
627 degassing from the main magma chamber would lead to increased pressure in the shallow aquifers
628 forming the large hydrothermal system, just as hypothesized for recent unrest (Moretti et al., 2017;

2018); moreover, the rise in temperature would cause the water contained in the tuffs' zeolites to convert into steam, generating additional overpressure. Such a situation is shown by the CF-23 well, where its stratigraphy indicates the presence of a magmatic layer approximately 30 m thick beneath the overlying tuff blocks, which are approximately 1.5 km thick (Fig. 14b).

It is noteworthy, when considering the correct stratigraphy of the resurgent block as represented by the CF-23 well, that some previous models suggesting the presence of two low-permeability layers at depth (Vanorio and Kanitpanyacharoen, 2015; Kilburn et al., 2023), inferred from the SV1 well (which is situated outside of the resurgent block) (Fig. 14a), can be questioned. Therefore, magmatic gases may not necessarily be restricted to below the thermo-metamorphic horizon (Kilburn et al., 2023), but may instead accumulate at shallower levels beneath the “summit” magma intrusion at a depth of about 2.5-3.0 km.”. Consequently, at the base of the magma body, conditions of high temperature and pressure result in widespread brittle deformation of this layer due to uplift, making it highly permeable by fracturing (Fig. 16b).

Finally, super-compressed magmatic gases were likely contained within an approximately 2.5 km thick fragile zone, while a limited release of the increased pressure occurred directly through the fractures connecting the intermediate depth area with the Solfatara and Pisciarelli areas, resulting in the escape of CO₂-rich vapor. A similar mechanism has been evidenced in the recent unrest, by the reported increase in fumarolic activity and in the CO₂/H₂O ratio (Chiodini et al. 2021).

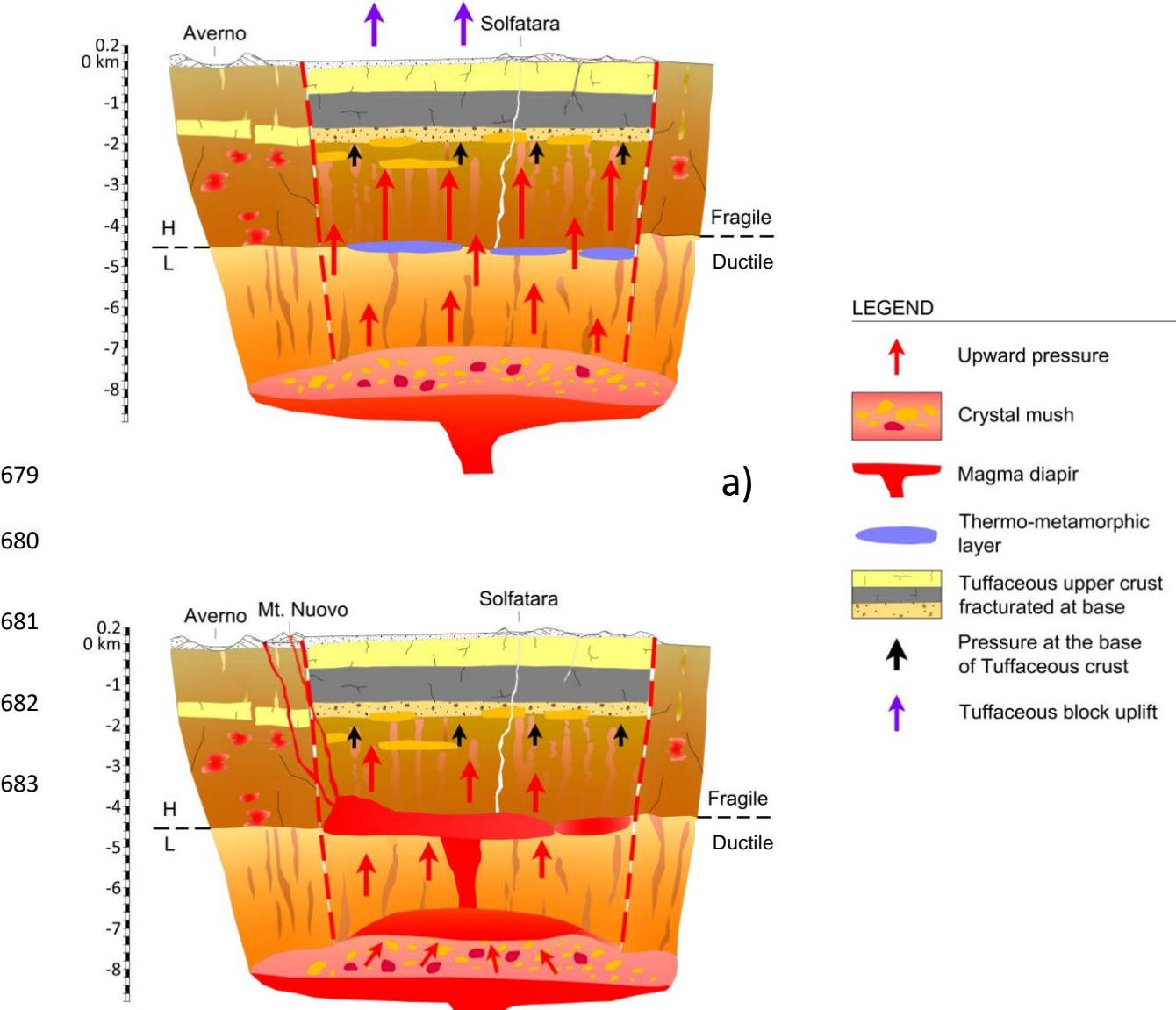
Following this hypothesis, it is noteworthy that, at a depth of 1.8 km, the CF23 drill-hole indicates a very high temperature of 300°C, not far from the supercritical temperature. It is plausible that, if the temperature significantly increases, due to the supply of deeper, hot magmatic fluids, the water contained in the basal part of the tuff block could reach supercritical conditions, leading to thermal fracturing within the tuff block (Vinciguerra et al., 2006), over a certain thickness (Fig. 16b).

As previously mentioned, the increase of pressure resulting from such intense heating caused by deeper magmatic fluids should be attributed to both the overpressure of shallow aquifers and the vaporization of water contained in the zeolites, likely in the form of superheated steam.

655

The pressure increase in the main magma chamber, resulting from the input of new magma and/or magmatic fluids as explained, can also trigger the formation of magma dykes (Troise et al., 2019). The progressive intrusion of several magma dykes likely leads to the ascent of magma towards the surface. This process may be further facilitated by phreatic explosions caused by the heating of shallow aquifers, resulting in depressurization pulses. Intruding magma may encounter layers that are more resistant to penetration at certain depths. In this case further magma intrusion may be inhibited and lateral expansion, to form sills, may occur (Gretener, 1969). Previous studies of recent unrests

663 have indicated that depths between 2.5 and 4 km, close to the upper limit of the ductile zone, are
 664 locations where magma intrusions can halt (Woo and Kilburn, 2010; Troise et al., 2019). Before the
 665 1538 eruption, a small plumbing system, in the form of flattened intrusions near the contact between
 666 a lower ductile zone and an upper brittle zone in a high-pressure environment, was hypothesized (Fig.
 667 16b) (Pasquarè et al., 1988). From such a shallower magma chamber, magma can further progress
 668 upward towards the surface. A dynamic in which early intrusions in the shallow crust create small
 669 plumbing systems (i.e. stalled intrusions), from which a dyke later propagates, bringing a small
 670 quantity of magma to the surface, is typical of monogenic volcanoes (Marti et al., 2016). The ability
 671 of intruded magma sills to erupt at surface is also influenced by the relatively short timescale of sill
 672 solidification, typically in the order of few tens of years (Troise et al., 2019).
 673 Shallow solidified magma sills, in the form of mush, can be remobilized due to the arrival of new
 674 magma and/or of hot deeper magma fluids. The significant uplift preceding the 1538 eruption,
 675 amounting to more than 16 meters in the initial phase involving the entire resurgent block, if
 676 interpreted solely in terms of magma intrusion, would suggest a total intruded volume, in the shallow
 677 plumbing system, on the order of some cubic kilometers of magma (Bellucci et al., 2006).
 678



684

685

686

687 **Fig. 16 – Schematic cross sections of the hydrothermal and magmatic systems underlying the**
688 **Campi Flegrei resurgent block in the 1538 AD, showing:**

689 **a) Process of gas sparging according to Bachmann and Bergantz (2006) model, related to the**
690 **transfer of hot gas from a mafic intrusion underplating the trachytic mush and the hypothesized**
691 **relation with earthquake swarms of the exsolved fluids, accumulated at lithostatic pressures in**
692 **the ductile region and episodically injected into the brittle crust at very high strain rates. The**
693 **sudden increase of fluid pressure, in the brittle region, can trigger earthquake swarms in the 2-**
694 **4 km depth range.**

695 **b) Remobilization of mush by mafic magmas then occurs, so the magma remobilized from the**
696 **mush accumulates at the top, fueling its rise upward to accumulate, in a sill-like shape, along**
697 **the ductile-brittle transition surface. Eruption from the magma sill is then likely to occur at the**
698 **faulted borders of the resurgent block.**

699

700 However, despite such a large uplift, suggesting however high volumes of shallow intruded magma,
701 the eruption of 1538 only produced about 0.03 km³ of pyroclastic deposits (see next section). This
702 discrepancy likely suggests that multiple sill intrusions occurred over more than one century, with
703 most of them solidifying without contributing to the eventual eruption. Only the most recent intrusion
704 events, and/or some portion of magma mush from prior intrusions remobilized by subsequent heating,
705 would have fed the eruption.

706 Also interesting is to note that, after the 1538 eruption, ground subsidence recovered only 8 meters,
707 i.e. one half of the former total ground uplift. This means that about one half of the total uplift was
708 likely caused by thermally pressurized gas and water (shallow aquifers), perturbed by hot fluids
709 coming from the deeper (7-8 km) magma chamber; the remaining, unrecovered uplift, should have
710 been caused by shallow magma intrusion. It is the same process hypothesized for recent unrests: in
711 particular, the 1982-1984 uplift showed a subsequent subsidence about one half than the former uplift,
712 interpreted as the deflation of formerly pressurized water and gas (Troise et al., 2019).

713 Another characteristic of eruptions from small monogenic volcanoes is their difficulty to be
714 forecasted, as they occur at unexpected locations (Marti et al., 2016). Both distinctive traits were
715 evident in the eruption of Monte Nuovo, which represents a prototype of a small monogenic volcano

716 in the Campi Flegrei. Despite the relatively small volume of magma (0.03 km^3), the eruption occurred
717 at a considerable distance, approximately three km westward, from the area of maximum uplift. The
718 position of the 1538 vent is approximately on the border of the resurgent block: such a border, marked
719 by ring faults, clearly represents a weak zone, where magma can more easily intrude.

720 **5.3 The eruption of 1538**

721 The week preceding the eruption was marked by a series of seismic events (Guidoboni and Ciuccarelli,
722 2011). The shoreline gradually retreated 200 steps (ca. 370m) seaward, because of an occasional uplift
723 occurred on the eastern shore of Lake Averno (see Fig. 2d) and during the 36 hours preceding the
724 eruption, the ground level reached 7 meters of total uplift (Parascandola, 1943; Costa et al., 2022). The
725 local uplift rapidly attenuated as a function of distance (Rolandi et al., 1985) (Fig. 6). The uplift,
726 involving a local marine regression, was accompanied by strong rumbles on the night between 28 and
727 29 September, culminated in a further explosion, at 2 am on the following night, which marked the
728 vent opening and the start of the eruption. The early eruptive column, initially white in colour, ejected
729 muddy ashes and lithic and scoriaceous lapilli upwards. The presence of wet ash on the slopes of the
730 gradually growing volcanic cone led Parascandola (1943) to hypothesize that it was a mud eruption.
731 This description, present in the chronicles of the time (Parascandola 1943), indicates that the first
732 eruptive phase was phreatomagmatic in character, although it evolved with a peculiar characteristic,
733 because the volcanic cone was formed by massive pyroclastic units, made up of loose and wet deposits,
734 ascribable to pyroclastic flows products with a prevalent sandy matrix, incorporating lithic and
735 scoriaceous clasts. In Fig. 17a we recognize three main flow units, each of them made up of sub-units.
736 These sub-units are mostly evident in the finest basal part (a), while in the intermediate part (b),
737 showing abundance of scoriaceous clasts, an inverse gradation is observed. Finally, the hydromagmatic
738 activity, lasted about 12 hours, built a small tuff cone, formed by successive waves of pyroclastic flow
739 units, whose deposits reached a height of approximately 120 m. This particular type of hydromagmatic
740 deposit implies an eruption in which the magma-water interaction process is characterized by a low
741 efficiency, considering the thermal energy of the magma and the mechanical energy generating the
742 eruption. In the classic Wohletz experimental diagram (Wohletz, 1983), besides the fields 1 and 3
743 which include, respectively, eruptions with zero or

744

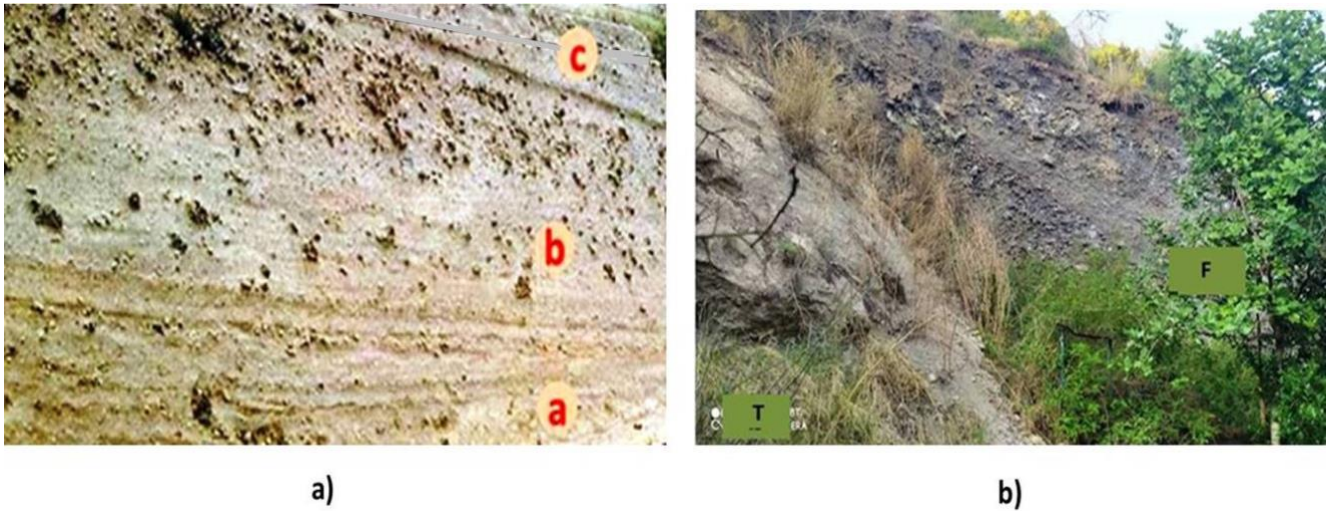


Fig. 17 – a) Flow units in the phreatomagmatic Pyroclastic flows, b) Deposit of the final scoria flow (F) in the western depression of the phreatomagmatic Tuff cone (T).

low magma/water ratio (0 – 0.1) and those with extremely high ratios (100-1000), field 2 includes hydro-magmatic explosive eruptions with an interaction ratio between 0.1 – 10, indicative of a greater value of mechanical efficiency (Fig. 18). It is evident, however, that even in field 2 there is a differentiation in efficiency, due to the condition characterizing the expansion of the water vapor that develops during the magma-water interaction process, that is:

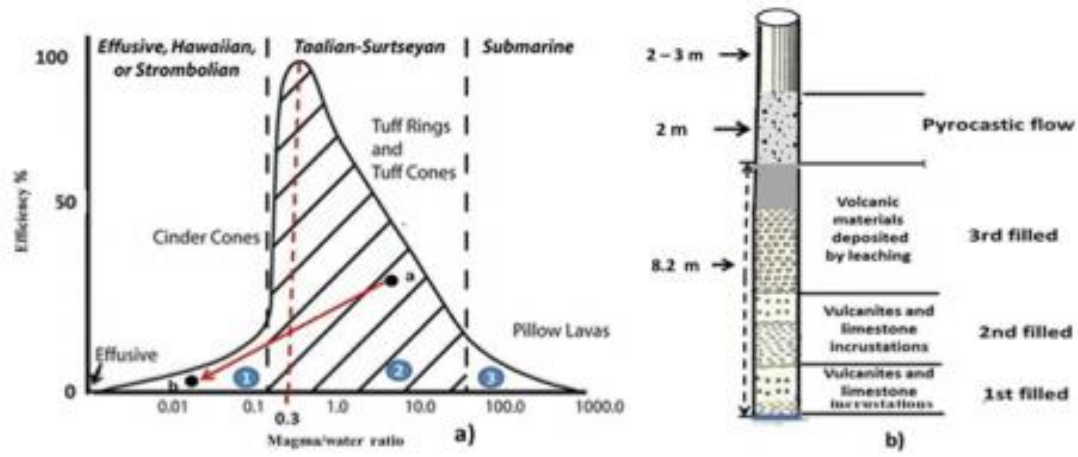
1) If the magma/water ratio is around the value of 0.3, the maximum efficiency is achieved. The quantity of water is optimal and expands entirely as superheated steam, that is, the maximum volume that can be generated is obtained without dispersing heat. Under this condition, the so-called Base Surges are formed;

2) If the water content increases, the efficiency drops because not all water is vaporized, and, as a result steam saturated with water is formed. Under this condition, Pyroclastic flows are formed.

This last type of flow is therefore associated with the collapsing eruptive column that developed in the night between 29 and 30 September, to be ascribed to a phreatomagmatic eruption with a high magma-water ratio, which gave rise to the non-welded ignimbrites described in typology 2 and located in the diagram of Fig.18a, at point a. Such particular condition for the flow, besides forming the new cone, also formed pyroclastic flows directed towards Pozzuoli. This kind of flow deposit, 5 m thick, is recognized in the tunnel of the new road to Arco Felice, located about 1 km from the cone (Fig.18c). These deposits, never described before, also easily explain the two meters of M. Nuovo eruption deposits described at Serapis Temple of Pozzuoli during the excavations (Parascandola, 1947), and formerly ascribed to fall products (fig.18b). This implied that in the initial phase of the eruption the magma absorbed a considerable quantity of sea water present above the eruptive vent, so in these

770 conditions, the collapsing eruptive columns which gave rise to the pyroclastic flows on the night
771 between the 29th and 30th September, reached a maximum height of less than 3 km, (Parascandola,
772 1943), depositing in a radius of approximately 3 km, as follows:

- 773 - with thickness of 5-10m, in sections obtained by cutting the slope in the area around the volcano (Fig.
774 17a);
- 775 - in a depression on the SE sector of the volcano. The materials of the Tuff Cone of Monte Nuovo (T)
776 are present, together with the products of the scoria flow (F) deposited in the SE depression (Fig. 17b).



778 **Fig. 18 – a) Wohletz (1983) diagram for the evaluation of the mechanical efficiency of the**
779 **products emitted in the form of Pyroclastic flows and fall/flow from Strombolian eruption**
780 **column collapse; b) products emitted by the 1538 eruption in the first eruptive phase as wet**
781 **pyroclastic flow, which buried the upper part of the Serapeum columns (above 8.2 m of height);**
782 **c) deposits of pyroclastic flow directed towards Pozzuoli, showing a thickness of about 5 m, in**
783 **the tunnel of the new road to Arco Felice**

784

785 According to the chronicles, on October 6th there was a new eruptive phase and 24 incautious visitors
786 died, surprised by the resumption of eruptive activity, which revealed itself with different
787 characteristics, mainly magmatic, that is, with a low water-magma interaction ratio (point b in Fig.
788 18a). In the hydromagmatic-magmatic transition, the eruptive cloud took the characteristic
789 ‘cauliflower’ shape of Strombolian eruptions, with a height of about 4 km, which, driven by winds
790 from the NW and then from the N, distributed the scoriaceous products towards the SE in the direction
791 of Nisida and the Neapolitan coast, then towards the S, in the direction of Bacoli and Capo Miseno
792 (Parascandola, 1943). The scoriaceous products of the second Strombolian magmatic eruptive phase
793 uniformly covered the basal units that formed the volcanic edifice during the first phase, with an
794 average thickness of about 0.5 m. The final phase of the eruption occurred with the collapse of the
795 Strombolian eruption column, which deposited a scoria flow in a depression on the eastern side of the
796 underlying cone of materials formed by phreatomagmatic pyroclastic flow units (Fig.17b). Overall,
797 the eruptive event of 1538, with the emission of 0.03 km^3 of pyroclastic material, can be classified
798 with a VEI = 2.

799

800 **3. The seismicity before and after the 1538 eruption**

801

802 The main precursors of the eruption, as reported by chronicles, were the earthquakes. Earthquake
803 sequences preceded, accompanied and followed the 1538 event. In this context, seismic precursors
804 may depend on the occurrence of stress perturbation, determined by the arrival of magmatic gases, as
805 well as directly by magma intruded at shallow crustal levels (typically at depth of 3-4 km), originating
806 from the main reservoir located at about 7.5-8.0 km depth.

807 We analyze here the earthquake sequences that occurred before the eruption. Earthquake magnitudes,
808 from inferred intensities of these earthquakes, have been computed as described in the Appendix 3.
809 We can then compare past earthquakes with those occurred during the recent unrests.

810

811

6.1 The seismic phases that accompanied the ground uplift and the eruption

We can classify the precursory earthquake sequences into three categories: long-term, medium-term and short-term precursors.

- The phase of *long-term seismic precursors* started in 1448 and was well documented since 1468 - 1470, when a paroxysmal seismic phase occurred ($I_o = VII$) (Guidoboni and Ciuccarelli, 2011; Francisconi et al., 2019) (Fig. 19a – interval A), resulting from a progressive increase in fracturing. This culminated into intense fumarolic-hydrothermal activity recorded at the Solfatara volcano. The historical chronicles report widespread damage to the vegetation, both spontaneous and cultivated, in all the areas surrounding the volcano. This appears to be an important piece of information, indicating a broadening of the area affected by intense degassing, (Francisconi et al., 2019). In 1475, another seismic phase was reported (Guidoboni, 2020), with maximum intensity $I_o = IV - V$. Over the following twenty years, ground uplift continued at an accelerated rate. This period culminated with a strong seismic phase occurring in October 1498, reaching considerable maximum intensity ($I_o = VII$). A low-intensity seismic phase then followed during the period 1499 - 1503 (maximum intensity $I_o = V$) (Fig. 19a – interval A). Such a long-term precursory phase could likely be interpreted as mainly due to intense degassing, coming from the deep magma chamber and progressively increasing pressure in the shallow layers of the geothermal system, without significant contribution from direct magma intrusion at shallow depth.

- After this first initial long-term precursory phase, a new phase of *medium-term precursors* followed. This phase was characterized by stronger seismic events in 1505 and 1508, which were of higher intensity with respect to the previous ones (maximum intensity $I_o = VIII$) (Guidoboni and Ciuccarelli, 2011). Additionally, there was a faster ground uplift during this period, resulting in serious damage to buildings and several casualties. This seismic phase could have been caused by either a higher stress associated with increased uplift level, or magma intrusion, from the deep magma chamber into shallower levels. This intrusion could have produced higher stress resulting in seismic activity of greater intensity. Although it is obviously difficult to identify, from historic sources alone, the respective roles of the deep degassing into the hydrothermal system versus shallow magma intrusion, we believe that the reported evidence of vegetation damage and increased degassing in the first phase, and the increase of earthquake intensity in the second phase, indicate respectively a main contribution of degassing perturbing the hydrothermal system, in the first phase, and of shallow magma intrusion in the second phase. This phase ended in 1520, with a medium intensity earthquake ($I_o = V-VI$) (Fig. 19a – interval B)..

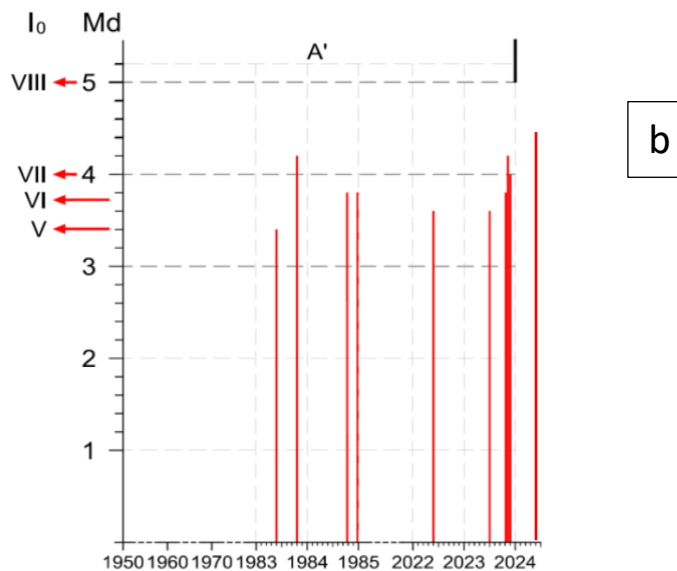
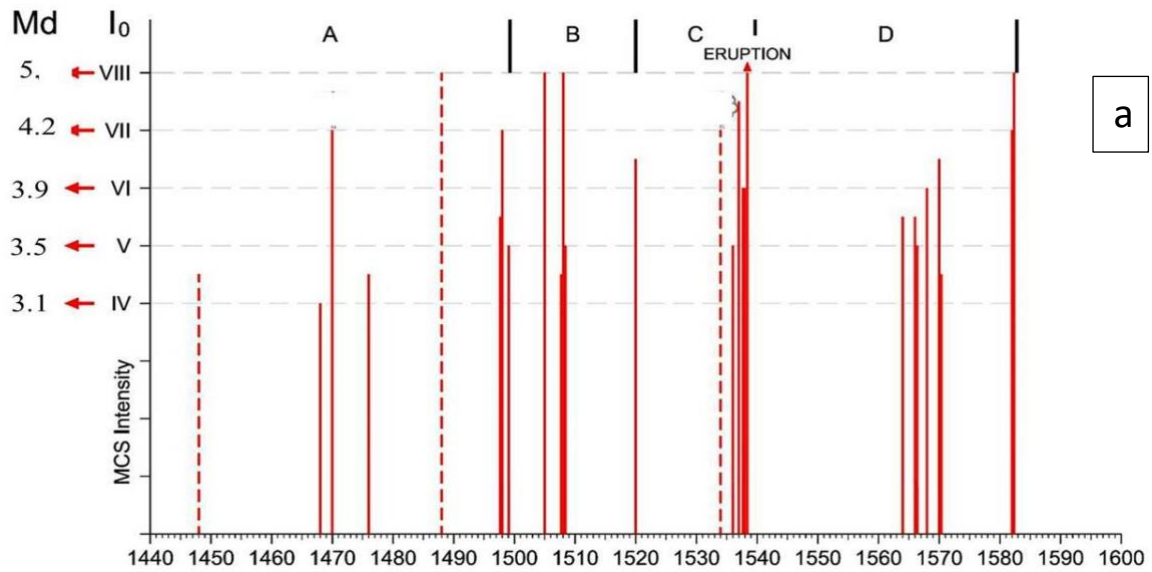


Fig. 19 – a) Reported earthquakes occurred before and after the 1538 eruption (after Guidoboni and Ciuccarelli, 2011). The computed intensities of these earthquakes have been converted in magnitudes using the considerations made in the appendix 3. b) Highest magnitude earthquakes ($M \geq 3.5$) occurred since 1950 to present.

After 16 years of relative seismic quiescence, likely characterized by low-intensity earthquakes not reported in chronicles, a short-term precursory phase began in 1536. It started with continuous seismicity, without major damage ($I_0 = \text{III} - \text{IV}$), continuing with similar features until the early 1537. It is possible that this last seismic phase, characterized by relatively low magnitude, was caused by low-frequency seismicity, resulting from magma oscillations during the fractures opening (see Chouet, 1996). This seismicity became more frequent just before the eruption. In February of the same year, the seismic activity peaked with stronger events ($I_0 = \text{VI} - \text{VII}$), accompanied by an

861 increase in the fumarolic activity at Solfatara. This provides evidence that this seismicity could be
862 again related to perturbations in the hydrothermal system. A final increase in seismic activity ($I_o =$
863 VIII), began in mid-June 1538, accompanied by a localized, significant additional ground uplift at
864 the eruption site, located 3 km away from the center of previous maximum uplift (Fig. 19a – interval
865 C) (Parascandola, 1943, Rolandi et al., 1986; Guidoboni and Ciuccarelli, 2011; Guidoboni, 2020).

866 -

867

868 **6.2 The post-eruption seismicity**

869 We will now consider the seismic phase following the eruption just described, which we will indicate
870 as the *aftereffect of the 1538 eruption*. This phase was likely triggered by continuing degassing from
871 the deep magma chamber, and/or by new episodes of shallow magma intrusion not reaching the
872 surface to erupt. It began in 1564 with earthquakes of medium intensity ($I_o = V - VI$), followed by a
873 phase of lower intensity 2 years later. In 1570 seismic intensity increased ($I_o = VI - VII$), causing
874 damage to the buildings of the city of Pozzuoli. Between 1575 and 1580 a new phase of low seismic
875 intensity began, culminating, in 1582, with two earthquakes, respectively of intensity $I_o = VII - VIII$.
876 These earthquakes caused partial collapses in several houses and serious damage to churches and
877 buildings, as well as numerous casualties (Parascandola, 1943; Guidoboni e Cucciarelli, 2010;
878 Guidoboni, 2020).

879

880 **4. Comparison of precursory phases of 1538 eruption with current unrest**

881 This study is mainly aimed at understanding how the evolution of the ground movement and seismicity
882 phases linked to the 1538 eruption can help build realistic scenarios for the evolution of the same recent
883 phases at the Campi Flegrei caldera. Common features between the medieval and present-day unrest
884 phases are described in the following:

885 The main similarity is that the seismicity, in the past and in the recent unrest, has been clearly correlated
886 both with the total uplift and the uplift rate; it is practically absent in periods of subsidence (Dvorak
887 and Gasparini, 1991; Kilburn et al., 2017; Troise et al., 2019).

888 We found, in particular, that seismicity of period 1950-2024 is on the same order than the period
889 1430-1503, whereas the latter, as we have previously observed, was the first phase of preparation of
890 the 1538 eruption. Although the total amount of uplift in the period 1430-1503, about 10 m, was more
891 than double than the total uplift recorded since 1950-2023, of about 4.1 m., the seismicity in the two
892 periods has been remarkably comparable. The maximum magnitude, $M=4.4$ recently occurred on
893 May 20th, 2024, is in fact very similar to the maximum magnitude reconstructed for the period 1430-
894 1503 (Fig.19a interval A and Fig.19b interval A').

895 It is also interesting to compare the average uplift rate before the 1538 eruption with that observed
896 since 1950 to present. In particular, we can compare the average uplift rate occurred in the first 70-
897 73 years, since 1430 to 1503, with that observed since 1950 till now. In the period 1430-1503
898 maximum ground uplift was about 10 m, thus implying an average uplift rate of about 13.5 cm/year;
899 actually, the average ground uplift since 1950 has been less than half: 6.1 cm/year. It is anyway
900 interesting to note that, in the last years, the continuous uplift period still ongoing is characterized by
901 an average uplift rate of about 12-20 cm/year.

902 Another common feature is that both seismic phases, as well as ground uplift, can be mostly ascribed
903 to the effect of pressurized hydrothermal fluids (Moretti et al., 2017; 2018; Troise et al., 2019). So,
904 till now there is a close analogy between the ‘long term precursory phase’ preceding the 1538 eruption
905 and the recent unrest 1950-2023; the only clear difference is, as we already noted, the much lower
906 cumulative uplift (and consequently average uplift rate) of the recent unrest.

907 Such observations led us to consider two possible scenarios for the evolution of the present unrest.

908

909 **7.1 First scenario**

910 The first scenario would imply that the present unrest progresses towards a new eruption. Although
911 there is, presently, no evidence for shallow magma intrusions occurring during the present unrest
912 since 2006 (see Moretti et al., 2017, 2018; Troise et al., 2019), a new shallow magma intrusion, in
913 the near future, cannot be ruled out. Another possibility is that the mush, which should be present at
914 low depth, could be re-mobilised by hot fluids coming from the main magma chamber, the way we
915 explained in the previous paragraphs. Troise et al. (2019), showed in fact evidence for a likely shallow
916 magma intrusion occurred at about 3 km of depth, during the 1982-1984 unrest, with a volume of
917 about 0.03 km³, i.e. the same order of magnitude of the erupted volume in the 1538 event. The same
918 authors calculated, in agreement with other authors (Woo and Kilburn, 2010; Moretti et al., 2013;
919 Moretti et al., 2018), that such a sill intrusion should have solidified, in form of mush, after about 20
920 years, i.e. around 2003. If the actual unrest will progress towards an eruption, it is also very likely
921 that seismicity will increase, in frequency and magnitude, possibly reaching magnitudes around 5 or
922 even higher. Earthquakes of magnitude 5, in this area, would occur at very shallow depths (not higher
923 than about 3 km), so producing high intensities (higher than VIII MCS, see Fig. 19). Finally, from a
924 civil protection perspective, we must also take into account the possible onset of a post-eruptive
925 seismic phase, which after the 1538 eruption lasted more than about 40 years. In conjunction with the
926 prefigured scenario, the problem of forecasting the position of a new eruptive vent is also extremely
927 relevant because, in principle, it could be opening in any sector of the caldera. Despite the indications
928 contained in several probabilistic studies on the subject (Alberico et al., 2002; Selva et al., 2011), we

929 must consider they are biased by the assumption of stationary conditions, which is implied in any
930 probability computation based on the frequency of past events; they just rely on the most frequent
931 vent locations of the past. As the most evident example that such probabilistic determinations have a
932 poor reliability, it is enough to note that, on the basis of similar calculations, the site of the 1538
933 Monte Nuovo eruption would have never been predicted. A more reliable indication of the most likely
934 future vent could come from the most seismic areas, because they reflect the areas of maximum shear
935 stress. In this perspective, the Solfatara-Agnano area (see Fig. 15a), which is by far the most
936 seismically active one, could be the most probable site for future vent opening. However, the most
937 effective way to address this problem would be the prompt determination of localized uplift in
938 addition to the usual bell-shaped one centered on Pozzuoli harbor. Although some recent eruptions
939 (e.g. at Hekla volcano: Wonderman, 2000) show that the rise of magma from several km to the surface
940 can be so fast to be practically useless for civil protection purposes, localized and considerable ground
941 uplift was actually observed before the 1538 eruption, making it likely that this precursor will be
942 observed before a future eruption in the area.

943 We must however consider the possibility that, even without new shallow magma intrusions, and/or
944 in absence of mobilized mush eruption, the increase of pressure for aquifer heating above the critical
945 threshold could produce a phreatic eruption. Phreatic eruptions are in general very difficult to
946 forecast, and also to detect from the past geological record. However, there is some robust indication
947 for at least one phreatic eruption occurred in the area, in 1198 (Scandone et al., 2010); it is also
948 realistic that most of the phreatomagmatic eruptions in the area started as phreatic eruptions, as
949 explained in previous paragraphs. The phreatic scenario deserves maximum attention for the current
950 evolution of the CF unrest, because of its serious implications for civil defense purposes, and for the
951 even higher difficulty to be forecasted, with respect to a magmatic eruption.

952

953 **7.2 Second scenario**

954 As an alternative scenario, we should consider the one which stops sometimes without evolving
955 towards an eruption. Despite the similarity of the recent unrest with the first phase leading to the 1538
956 eruption, we could in fact consider the notable difference in the cumulative uplift between the past
957 and present unrests: 10 m., as compared with less than 4.5 m. The level of ground uplift is critical,
958 because it indicates the level of stress accumulated underground. As pointed out by Kilburn et al.
959 (2017), when the level of stress reaches a critical value, the medium rheology becomes totally fragile
960 and any small amount of incremental stress can cause the collapse (i.e. the catastrophic fracturing) of
961 the shallow crust, thus producing the eruption. Actually, we don't know the critical stress level for
962 the shallow crust at Campi Flegrei. Kilburn et al. (2023) claimed, from the observation of the trend

963 of cumulative number of earthquakes as a function of cumulative uplift, that such critical value would
964 have been reached and overcome in 2015. Besides any speculation on their interpretations, it is clear
965 that, if the internal stress had really overcome the critical level in 2015, considering the large
966 additional uplift cumulated since then (about 0.90 m.), and hence the considerable incremental stress,
967 the system would have already collapsed, and an eruption occurred. The very high deformation
968 occurred before the 1538, namely 16 m plus the localized uplift occurred just at the vent site before
969 the eruption, seems to indicate that the critical stress level, at that time, was much higher than the one
970 presently reached. So, if it could be assumed the medium strength today is similar, there is a
971 possibility that the progression towards eruption conditions is too gradual to culminate in an actual
972 eruption, and the unrest may cease before reaching that point; or, however, that the time to reach the
973 critical stage will be much longer (200-250 years, instead of about 100).

974 5. Conclusion

975 In this paper, we have presented a detailed reconstruction of the ground deformation, and a
976 comprehensive analysis of the main observations characterizing the events before, during and after the
977 1538 Monte Nuovo eruption, the only eruption occurred at Campi Flegrei caldera in historical times.
978 This reconstruction, based on clear historical evidence, has allowed us to correct some widely diffused
979 but questionable reconstructions, found in the past and recent literature.. Specifically, we demonstrated
980 that subsidence in the area began, at least, during the Greek colonization (VIII century BC) and
981 persisted through Roman times, with documentation dating back to 90 BC. Additionally, we
982 reconstructed the evolution of ground deformation at Pozzuoli harbor during the Middle Age,
983 demonstrating that maximum subsidence occurred around 1430. We also tracked the ground level from
984 1430 until the first half of the 19th century, using historical data on the height of the Serapeum floor
985 relative to sea level.

986 Furthermore, by reconstructing the subsidence and uplift of the Via Herculea, based on ancient
987 chronicles, we provided clear evidence indicating that the local uplift preceding the eruption at the
988 Monte Nuovo site, situated near Via Herculea, did not exceed 5-7 meters, since Via Herculea never
989 re-emerged from sea before and during the eruption. This evidence disproves claims in recent literature
990 (Di Vito et al., 2016), that suggested local uplift around M. Nuovo reached elevations as high as 19 m
991 immediately before the eruption.

992 Our reconstruction of geophysical anomalies (mainly ground displacement and seismicity) preceding
993 and following the 1538 eruption has been tentatively interpreted in comparison with observations and
994 data collected during the recent unrests. This approach enables the formulation of two possible
995 scenarios for the evolution of the present unrest, which, so far, has shown notable similarities to the
996 long-term precursors of the 1538 eruption.

997 The first scenario involves the progression of phenomena towards an eruption, suggesting that, in the
998 near future, earthquakes with magnitude up to 5 or slightly higher may occur, both preceding the
999 eruption and persisting for several decades afterward. Conversely, the alternative scenario, implies that
1000 the unrest may cease before an eruption occurs. This possibility is supported by the fact that ground
1001 uplift observed from 1950 to 2024, compared with the uplift occurred over an equivalent period from
1002 1430 to 1503, is significantly lower (4.3 m as compared to 10 m). Since the overpressure in the system
1003 is somewhat proportional to the amount of uplift, it is plausible that the recent unrest has not reached
1004 the critical value for catastrophic fracture of shallow rocks. In addition, if cumulative stress increases
1005 too slowly, a substantial amount of previous stress can be cleared depending on viscoelastic relaxation
1006 and its characteristic times. While the exact critical threshold and viscoelastic relaxation time remain
1007 unknown, they can be tentatively inferred from the maximum deformation observed before the 1538
1008 eruption. The bell-shaped cumulative vertical displacement centered at Pozzuoli, before the 1538
1009 eruption, was much larger, reaching 16 m., compared to the about 4.5 m recorded from 1950 to 2024.
1010 This substantial difference, assuming the rheology and strength of shallow rocks in the 0-3 km depth
1011 range remain unchanged, would suggest that we are currently far from reaching the critical stress
1012 threshold necessary for an eruption.

1013 A further, important consideration, coming from the observation that pyroclastic flows from 1538
1014 reached the centre of Pozzuoli, is that even a very small eruption (as the 1538 one) can produce
1015 pyroclastic flows travelling some km on flat ground.

1016 Finally, this work put in evidence that the most critical events, with civil defense implications, we
1017 could reasonably expect in case of a future eruption, are the following:

- 1018 1) increasing seismic activity and M 5 events
- 1019 2) phreatic eruption
- 1020 3) phreatic eruption followed by a phreato-magmatic one
- 1021 3) pyroclastic flows travelling more than 3 km, inside the caldera, even in case of a small, VEI=2
1022 eruption like the 1538 one.

1023

1024 **Data availability**

1025 All raw data can be provided by the corresponding authors upon request.

1026

1027 **Author contributions**

1028 GR, GDN and CT analyzed historical and volcanological data; GDN and CT analyzed earthquake
1029 intensity/magnitude data; MS analyzed seismic data; GR, MS and MDL wrote the manuscript draft
1030 and prepared the figures; GDN, CT and MS reviewed and edited the manuscript.

1031
1032
1033
1034
1035
1036
1037
1038
1039

1040

1041
1042

1043
1044

1045
1046

1047
1048
1049

1050
1051
1052

1053
1054
1055

1056
1057
1058
1059

Competing interests

The authors declare that they have no conflict of interest.

Acknowledgments

The authors want to thank Prof. Marina Petrone who helped to recover some important Middle Age references on Campi Flegrei.

References

- Acocella V., 2010. Evaluating fracture patterns within a resurgent caldera: Campi Flegrei. Italy. Bull. Volcanol., 72, 623-638.
- Acocella V., 2019. Bridging the gap from caldera unrest to resurgence. Front. Earth Science, 7, 173. <https://doi.org/10.3389/feart.2019.00173>.
- AGIP, 1987. Geologia e geofisica del sistema geotermico dei Campi Flegrei. Servizi Centrali per l'Esplorazione, SERG-MMESG, San Donato
- Alberico, I., Petrosino, P., and Lirer, L., 2011. Volcanic hazard and risk assessment in a multi-source volcanic area: the example of Napoli city (Southern Italy), Nat. Hazards Earth Syst. Sci., 11, 1057–1070, <https://doi.org/10.5194/nhess-11-1057-2011>, 2011.
- Altaner, S., Demosthenous, C., Pozzuoli, A., Rolandi, G., 2013. Alteration history of Mount Epomeo Green Tuff and a related polymictic breccia, Ischia Island, Italy: Evidence for debris avalanche. Bulletin of Volcanology 75, 5, <https://doi.org/10.1007/s00445-013-0718-1>
- Amato, L. and Gialanella, C., 2013. New evidences on the Phlegraean bradyseism in the area of Puteolis harbour. Conference: Geotechnical Engineering for the Preservation of Monuments and Historic Sites. <https://doi.org/10.13140/2.1.2326.0482>
- Amoruso, A., Crescentini, L., Berrino, G., 2008. Simultaneous inversion of deformation and gravity changes in a horizontally layered half-space: Evidences for magma intrusion during the 1982–1984 unrest at Campi Flegrei caldera (Italy). Earth Planet. Sci. Lett., 272, 181–188. <https://doi.org/10.1016/j.epsl.2008.04.040>.

1060 Amoruso, A., Crescentini, L., Sabetta, I., 2014. Paired deformation sources of the Campi Flegrei
 1061 caldera (Italy) required by recent (1980–2010) deformation history. *J. Geophys. Res.*, 119, 858–879.
 1062 <https://doi.org/10.1002/2013JB010392>.

1063 Anecchino, R., 1931. Agnano, l'origine del nome e del lago. *Bollettino Flegreo*, 5.
 1064

1065 Aster, R. and Meyer, R., 1988. Three-dimensional velocity structure and hypocenter distribution in
 1066 the Campi Flegrei caldera, Italy. *Tectonophysics*, 149, 195–218
 1067

1068 Aucelli, P.C. et al., 2020. Ancient Coastal Changes Due to Ground Movements and Human
 1069 Interventions in the Roman Portus Julius (Pozzuoli Gulf, Italy): Results from Photogrammetric and
 1070 Direct Surveys. *Water*, 12, 658. <https://doi.org/10.3390/w1203065>

1071 Bachmann, O., Bergantz, G.W., 2006. Gas percolation in upper-crustal silicic crystal mushes as a
 1072 mechanism for upward heat advection and rejuvenation of near-solidus magma bodies. *Journ.*
 1073 *Volcanol. and Geoth. Res.*, 149, 85–102
 1074

1075 Bachmann, O., Huber, C., 2016. Silicic mushes reservoirs in the Earth's crust. *American*
 1076 *Mineralogist*, 101, 11, 2377–2404. <https://doi.org/10.2138/am-2016-5675>
 1077

1078 Barberi, F., Corrado, G., Innocenti, F., Luongo, G., 1984. Phlegraean Fields 1982–1984: Brief
 1079 Chronicle of a Volcano Emergency in a Densely Populated Area. *Bull. Volcanol.*, 47-2, 175–185.

1080 Bergantz, G.W., 1989. Underplating and partial melting: implications for melt generation and
 1081 extraction. *Science* <https://doi.org/10.1126/science.245.4922.1093>

1082 Berrino, G., Corrado, G., Luongo, G., Toro, B., 1984. Ground deformation and gravity changes
 1083 accompanying the 1982 Pozzuoli uplift. *Bull. Volcanol.*, 44-2, 187–200.

1084 Bianchi, R., Coradini, A., Federico, C., Giberti, G., Lanciano, P., Pozzi, J.P., Sartoris, G., Scandone,
 1085 R., 1987. Modeling of surface deformation in volcanic areas: The 1970–1972 and 1982–1984 crises
 1086 of Campi Flegrei, Italy. *J. Geophys. Res.*, 92, B13, 14139–14150. Brahm, R., Parada,
 1087 M.A., Morgado, E.E., Contreras, C., 2015. Pre-eruptive rejuvenations of crystalline mush by
 1088 reservoir heating: the case of trachy-dacitic lavas of Quetupillán Volcanic Complex, Chile (39°30'
 1089 lat. S). *American Geophysical Union, Fall Meeting 2015*, abstract id. V43B-3122, Bibcode:
 1090 2015AGUFM.V43B3122B

1091

1092 Burgisser, A., Bergantz, G.W., 201. A rapid mechanism to remobilize and homogenize crystalline
1093 magma bodies. *Nature* 471(7337):212-5, <https://doi.org/10.1038/nature09799>

1094

1095 Battaglia, J., Zollo, A. Virieux, J., Dello Iacono, D., 2008. Merging active and passive data sets in
1096 travelttime tomography: The case study of Campi Flegrei caldera (Southern Italy) *Geophysical*
1097 *Prospecting*, 56, 555–573 <https://doi.org/10.1111/j.1365-2478.2007.00687.x>

1098 Bellucci, F., Woo, J., Kilburn, C. R. J. & Rolandi, G., 2006. In *Mechanisms of Activity and Unrest*
1099 *at Large Calderas Vol. 269* (eds. Troise C., De Natale, G. & Kilburn, C.R.J.) *The Geological Society*
1100 *of London Special Publication*, 141–158.

1101 Beauducel, F., De Natale, G., Obrizzo, F., Pingue, F., 2004. 3-D modelling of Campi Flegrei ground
1102 deformations: role of caldera boundary discontinuities. *Pure Appl. Geophys.*, 161.

1103 Boccaccio, G., 1355-1373. *De Montibus*.

1104 Bodnar, R. J., Cannatelli, C., de Vivo, B., Lima, A., Belkin, H.E., Milia, A., 2007. Quantitative model
1105 for magma degassing and ground deformation (bradyseism) at Campi Flegrei, Italy: implications for
1106 future eruptions, *Geology*, 35, 9, pp. 791–794.

1107 Calò, M., Tramelli, A., 2018. Anatomy of the Campi Flegrei caldera using enhanced seismic
1108 tomography models, *Scientific Reports*, 8, 1, 16254.

1109 Camodeca, G., 1987. *Le antichità di Pozzuoli, la Ripa Puteolana e i resti sommersi del Porto Giulio*,
1110 G. Macchiaroli Editore, Napoli.

1111 Cannatelli, C., Spera, F.J., Bodnar, R.J., Lima, A., De Vivo, B., 2020. Ground movement
1112 (bradyseism) in the Campi Flegrei volcanic area: a review. In: “Vesuvius, Campi Flegrei, and
1113 Campanian volcanism”, In: De Vivo B., Belkin H. E & Rolandi G., Eds, Elsevier, 15, 407-433. ISBN:
1114 978-0-128-16454-9.

1115

1116 Cappelletti, P., Petrosino, P., De Gennaro, M., Colella, A., Graziano, S.F., D’Amore, M., Mercurio,
1117 M., Cerri, G., De Gennaro, R., Rapisardo, G., Langella, A., 2015. The “Tufo Giallo della Via
1118 Tiberina” (Sabatini Volcanic District, Central Italy): a complex system of lithification in a pyroclastic

1119 current deposit. Mineralogy and Petrology, 109 (1) 85-101 <https://doi.org/10.1007/s00710-014-0357->
1120 z
1121
1122 Carrara, A., Burgisser, A., Bergantz, G.W., 2020. The architecture of intrusions in magmatic mush.
1123 Earth and Planetary Science Letters, 549, 1, 116539.

1124 Caricchi, L., Annen ,C., Blundy, J.D., Simpson, G., Pinel, V., 2014. Frequency and magnitude of
1125 volcanic eruptions controlled by magma injection and buoyancy. Nature Geoscience, 7, 126–
1126 130. <https://doi.org/10.1038/ngeo2041>.

1127 Caruso, M., 2004. Il territorio puteolano fra età romana e alto Medioevo. Bollettino Flegreo, Terza
1128 serie, N°17

1129 Cashman, K.V., Sparks, R.S.J., Blundy, J., 2017. Vertically extensive and unstable crystals mushes:
1130 a unifying view of igneous processes associated with volcanoes. Science 355, 6331,
1131 <https://doi.org/10.1126/science.aag3055>

1132 Charlton, D., Kilburn, C., Edwards, S., 2020. Volcanic unrest scenarios and impact assessment at
1133 Campi Flegrei caldera, Southern Italy. Journal of Applied Volcanology, 9, 7 (DOI).

1134

1135 Chiodini, G., Vandemeulebrouck, J., Caliro, S., D'Auria, L., De Martino, P., Mangiacapra, A.,
1136 Petrillo, Z., 2015. Evidence of thermal driven processes triggering the 2005-2014 unrest at Campi
1137 Flegrei caldera. Earth Planet. Sci. Lett., 414, 58-67. <https://doi.org/10.1016/j.epsl.2015.01.012>.

1138 Chiodini, G., Caliro, S., Avino, R. et al., 2021. Hydrothermal pressure-temperature control on CO2
1139 emissions and seismicity at Campi Flegrei (Italy),” Journal of Volcanology and Geothermal Research,
1140 414, 107245. <https://doi.org/10.1016/j.jvolgeores.2021.107245>.

1141

1142 Chouet, B. A. (1996). Long-period volcano seismicity: its source and use in eruption
1143 forecasting. Nature, 380, 6572, 309-316. <https://doi.org/10.1038/380309a0>

1144

1145 Cinque, A., Rolandi, G., Zamparelli, V., 1983. L'estensione dei depositi marini olocenici
1146 nei Campi Flegrei in relazione alla vulcanotettonica. Boll. Soc. Geol. It, 104, 327-348

1147

1148 Colletta, T., 1988. Pozzuoli, città fortificata in epoca vicereale - Storia dell'Urbanistica/Campania 1-
1149 Pozzuoli. Pubblicazione semestrale diretta da E. Guidoni. Supplemento Luglio-Dicembre

1150

1151 Costa, A., Di Vito, M.A, Ricciardi, G.P., Smith, V. C., Talamo, P., 2022. The long and intertwined
1152 record of humans and the Campi Flegrei volcano (Italy). Bulletin of Volcanology, 84, 5.
1153 <https://doi.org/10.1007/s00445-021-01503->

1154 D’Antonio, M., Civetta, L., Orsi, G., Pappalardo, L., Piochi, M., Carandente, A., De Vita, S.,
1155 Di Vito, M.A., Isaia, R., 1999. The present state of the magmatic system of the Campi Flegrei
1156 caldera based on a reconstruction of its behavior in the past 12 ka. J. Volcanol. Geotherm.
1157 Res., 91, 2-4, 247-268.

1158 De Jorio, A., 1820. Ricerche sul Tempio de Serapide in Pozzuoli, Monumenti inediti di Antichità e
1159 Belle Arti, Napoli.

1160 Del Gaudio, C., Aquino, I., Ricciardi, G.P., Ricco, C., Scandone, R., 2010. Unrest episodes at Campi
1161 Flegrei: A reconstruction of vertical ground movements during 1905–2009. Journal of Volcanology
1162 and Geothermal Research 195, 1, 48-56. <https://doi.10.1016/j.jvolgeores.2010.05.014>

1163 De Natale, G., Zollo, A., 1986. Statistical analysis and clustering features of the Phlegraean Fields
1164 earthquake sequence (May 1983-May 1984). Bull. Seism. Soc. Am., 76, 3, 801–814.
1165 <https://doi.org/10.1785/BSSA0760030801>

1166

1167 De Natale, G., Pingue, F., Allard, P. and Zollo, A., 1991. Geophysical and geochemical modeling of
1168 the Campi Flegrei caldera. In ‘*Campi flegrei*’ (G. Luongo R. Scandone eds.), J. Volcanol. Geotherm.
1169 Res., 48, 199–222.

1170

1171 De Natale, G., Pingue, F., 1993. Ground deformations in collapsed caldera structures. Journal of
1172 Volcanology and Geothermal Research, 57, 1-2, 19-38.

1173

1174 De Natale, G., Petrazzuoli, S.M., Pingue, F., 1997. The effect of collapse structures on ground
1175 deformations in calderas. Geophysical Research Letters, 24, 1555–1558.

1176

1177 De Natale, G., Troise, C., Pingue, F., 2001. A mechanical fluid-dynamical model for ground
1178 movements at Campi Flegrei caldera. J. Geodyn., 32, 487-517.

1179

1180 De Natale, G., Kuznetov, I., Krondrod, T., Peresan, A., Sarao, A., Troise, C., Panza, G.F., 2004.
 1181 Three decades of seismic activity at Mt. Vesuvius: 1972-2000. *Pure Appl. Geophys.*, 161, 1, 123-
 1182 144. <https://doi.org/10.1007/s00024-003-2430-0>
 1183
 1184 De Natale, G., Troise, C., Pingue, F., Mastrolorenzo, G., Pappalardo, L., Battaglia, M., Boschi, E.,
 1185 2006b. The Campi Flegrei caldera: Unrest mechanisms and hazards. (London: Geological Society)
 1186 *Geol. Soc. London Spec. pub.*, 269, 1. <https://doi.10.1144/GSL.SP.2006.269.01.03>.
 1187
 1188 De Natale, G., Troise, C., Mark, D., Mormone, A., Piochi, M., Di Vito, M.A., Isaia, R., Carlino, S.,
 1189 Barra., D., Somma, R., 2016. The Campi Flegrei Deep Drilling Project (CFDDP): New insight on
 1190 caldera structure, evolution and hazard implications for the Naples area (Southern Italy).
 1191 *Geochemistry, Geophysics, Geosystem*, <https://doi.org/10.1002/2015GC00618341>.
 1192
 1193 De Natale, G., Petrazzuoli, S., Romanelli, F., Troise, C., Vaccari, F., Somma, R., Peresan, A., Panza,
 1194 G.F., 2019. Seismic risk mitigation at Ischia island (Naples, Southern Italy): an innovative approach
 1195 to mitigate catastrophic scenarios. *Eng. Geol.*, 261, 105285.
 1196
 1197 Di Bonito, R., Giamminelli, R., 1992. *Le Terme dei Campi Flegrei, Topografia Storica*. Jandi Sapi
 1198 Editori, Milano-Roma.
 1199
 1200 Di Girolamo, P., Ghiara, M.R., Lirer, L., Munno, R., Rolandi, G., Stanzione, D., 1984.
 1201 *Vulcanologia e petrologia dei Campi Flegrei*. *Boll. Soc. Geol. Ital.*, 103.
 1202
 1203 Di Vito, M.A., Lirer, L., Mastrolorenzo, G., Rolandi G., 1987. The Monte Nuovo eruption (Campi
 1204 Flegrei, Italy). *Bulletin of Volcanology* 49, 608–615.
 1205
 1206 Di Vito, M.A., Isaia, R., Orsi, G., Southon, J., De Vita, S., D’Antonio, M., Pappalardo, L., Piochi,
 1207 M., 1999. Volcanism and deformations since 12.000 years at Campi Flegrei caldera
 1208
 1209 Di Vito, M.A., Arienzo, I., Braia, G., Civetta, L., D’Antonio, M., Di Renzo, V., Orsi, G., 2011. The
 1208 Averno 2 fssure eruption: a recent small-size explosive event at the Campi Flegrei caldera (Italy).
 1209 *Bull. Volcanol* 73:295–320. <https://doi.org/10.1007/s00445-010-0417>

1210 Di Vito, M.A., Acocella, V., Aiello, G., Barra, D., Battaglia, M., Carandente, A., Del Gaudio, C., S.
 1211 de Vita, S., GP Ricciardi, G.P., Ricco, C., Scandone, R., Terrasi, F., 2016. Scientific Reports, 6,
 1212 Article number: 32245. <http://www.nature.com/articles/srep32245>

1213 Dvorak, J.J. and Gasparini, P., 1991. History of earthquakes and vertical ground movement in Campi
 1214 Flegrei caldera, Southern Italy: comparison of precursory events to the A.D. 1538 eruption of Monte
 1215 Nuovo and of activity since 1968. Journ. Volc. Geoth. Res., 48, 1-2.
 1216

1217 Dvorak, J.J., Mastrolorenzo, G., 1991. The mechanism of recent movements in Campi Flegrei
 1218 caldera, Southern Italy. Geologic Society of America special paper, 263.

1219 Druitt, T.H., Sparks, R.S.J., 1984. On the formation of calderas during ignimbrite eruptions. Nature,
 1220 310, 679-681.

1221 Edmonds, M., Cashman, K. V., Holness, M., Jackson, M., 2019. Architecture and dynamics of
 1222 magma reservoirs. Phil. Trans. Royal Soc., Mat. Phis. and engeener. Sci., 377, 2139.
 1223 <https://doi.org/10.1098/rsta.2018.0298>

1224

1225 Folch, A., Gottsmann, J., 2006. Faults and ground uplift at active calderas, Geological Society,
 1226 London, Special Publications, 269, 109–120.
 1227

1228 Fournier, R.O., 1999. Hydrothermal processes related to movement of fluid from plastic into brittle
 1229 rock in the magmatic epithermal environment, Econ. Geol., 94, 8, 1193-1211.
 1230

1231 Francisconi, G., Todesco, M., Ciuccarelli, C., 2019. Storia del Monte Nuovo. L'ultima eruzione dei
 1232 Campi Flegrei. INGV Vulcani.
 1233

1234 Franco, E., 1974. La zeolitizzazione naturale: in zeoliti e zeolitizzazione. Atti Convegni Licei, 33-60

1235 Fuiano, M., 1951. Niccolò Jamsilla. Atti dell'Accademia Pontaniana. Nuova serie, Volume 3 – Anno
 1236 Accademico 1949 -50 – Napoli - Stabilimento tipografico Giannini

1237 Gaeta, F.S., Peluso, F., Milano, G., Arienzo, I., 2002. A Physical Appraisal of A New Aspect of
 1238 Bradyseism: The Mini-uplifts. Journal of Geophysical Research Atmospheres 108(B8)
 1239 <https://doi.org/10.1029/2002JB001913>

1240

1241 Gianfrotta, P.A., 1993. Puteoli sommersa, in F. Zevi (a cura di), Puteoli: 115-124. Napoli, Banco di
1242 Napoli.

1243 Gudmundsson, A., 2012. Magma chambers: Formation, local stresses, excess pressures, and
1244 compartments. *Jour. Volcanol. Geoth. Res.*, <https://doi.org/10.1016/j.jvolgeores.2012.05.015>

1245

1246 Guidoboni, E., Ciuccarelli, C., 2011. The Campi Flegrei caldera: historical revision and new data on
1247 seismic crises, bradyseisms, the Monte Nuovo eruption and ensuing earthquakes (twelfth century
1248 1582 AD), *Bulletin of Volcanology*, 73, 6, pp. 655-677, <https://doi.org/10.1007/s00445-010-0430-3>

1249 Guidoboni, E., 2020. Pozzuoli - terremoti e fenomeni vulcanici nel lungo periodo. a cura di AISI-
1250 Associazione Italiana di Storia dell'Ingegneria - VIII Convegno di Storia dell'Ingegneria, Napoli,
1251 Volume I

1252 Gretener, P.E., 1969. On the mechanics of the intrusion of sills. *Canadian Journal of Earth Sciences*,
1253 6, 6.

1254 Gauthier, V., 1912. Il Bradisisma Flegreo all'epoca ellenica. *Rend. Real Accad. Sci, Fis. e Mat.*
1255 Napoli, Serie III, Vol. XVIII, Anno LI, 91-94.

1256

1257 Iervolino, I., Cito, P., De Falco, M. *et al.*, 2024. Seismic risk mitigation at Campi Flegrei in volcanic
1258 unrest. *Nat. Commun.* 15, 10474. <https://doi.org/10.1038/s41467-024-55023-1>

1259 Isaia, R., Vitale, S., Di Giuseppe, M.G., Iannuzzi, E., D'Assisi Tramparulo, F., Troiano, A., 2015.
1260 Stratigraphy, structure, and volcano-tectonic evolution of Solfatara maar-diatreme (Campi Flegrei,
1261 Italy). *GSA Bulletin*, 127, 9-10, 1485–1504. <https://doi.org/10.1130/B31183.1> Johnson, E.R.,
1262 Wallace, P.J., Cashman, K.V., Granados, H.D., Kent, A.J.R., 2008. Magmatic volatile contents and
1263 degassing-induced crystallization at Volcán Jorullo, Mexico: Implications for melt evolution and the
1264 plumbing systems of monogenetic volcanoes. *Earth Plan. Sci. Lett.*, 269, 477

1265

1266 Kilburn, C.R.J., De Natale, G., Carlino, S., 2017. Progressive approach to eruption at Campi Flegrei
1267 caldera in southern Italy. *Nature Communications*, 8, 15312

1268 Kilburn, C.R.J., Carlino, S., Danesi, S., Pino, N.A., 2023. Potential for rupture before eruption at
 1269 Campi Flegrei caldera, Southern Italy. *Commun. Earth Environ.*, 4, 190.
 1270 <https://doi.org/10.1038/s43247-023-00842-1>

1271 Lanzarin, O., 2021. Trugli dei bagni di Pozzuoli. Immagine e fortuna di due edifici termali antichi.
 1272 <https://doi.org/10.17401/lexicon.33.2021-i>

1273 Lima, A., De Vivo, B., Spera, F.J. et al., Bodnar, M., Milia, A., Nunziata, C., Belkin, H., Cannatelli,
 1274 C., 2009. Thermodynamic model for uplift and deflation episodes (bradyseism) associated with
 1275 magmatic-hydrothermal activity at the Campi Flegrei (Italy). *Earth Sci. Rev.*, 97, 1-4, 44–58.

1276 Lima, A., Bodnar, R.J., De Vivo, B., Spera, F. J., Belkin, H.E., 2021. Interpretation of Recent Unrest
 1277 Events (Bradyseism) at Campi Flegrei, Napoli (Italy): Comparison of Models Based on Cyclical
 1278 Hydrothermal Events versus Shallow Magmatic Intrusive Events. *Geofluids* , 2000255.
 1279 <https://doi.org/10.1155/2021/2000255>.
 1280

1281 Luongo, G., Cubellis, E., Obrizzo, F., Petrazzuoli, S.M., 1991. The mechanics of the Campi Flegrei
 1282 resurgent caldera: a model. *Journ. Volcan. Geotherm. Res.*, 45, 3–4, 161-172.

1283 Mancusi, F., 1987. Campi Flegrei. Sergio Civita Editore, Napoli.
 1284

1285 Marti, J., Lopez, C., Bartolini, S., Becerrill, L., 2016. Stress control of monogenic volcanism: A
 1286 review. *Front. Earth Sci., Sec. Volcanology*, 4
 1287

1288 Marturano, A., Esposito, E., Porfido, S., Luongo, G., 1988. Il terremoto del 4 Ottobre 1983
 1289 (Pozzuoli): Attenuazione dell'intensità con la distanza e relazione magnitudo-Intensità, zonazione
 1290 della città di Napoli. *Mem. Soc. Geol. It.*, 41, 941-948

1291

1292 Marsh, B.D., 1989. Magma chambers. *Ann. Rev. Earth Planet Sci.* 17, 439–474.
1293 <https://doi.org/10.1146/annurev.ea.17.050189.002255>

1294

1295 Milana, G., De Sortis, A., Rovelli, A., 2010. Contenuto in bassa frequenza nei terremoti vulcanici del
1296 Monte Etna e danneggiamento degli edifici. Fascicolo N.2: Progettazione Sismica, Sezione Articoli
1297

1298 Moretti, R., Orsi, G., Civetta, L., Arienzo, I., Papale, P., 2013. Multiple magma degassing sources at
1299 an explosive volcano. *Earth Planet. Sci. Lett.*, 367, 95-104.
1300 <https://doi.org/10.1016/j.epsl.2013.02.013>.

1301

1302 Moretti, R., De Natale, G., Troise, C., 2017. A geochemical and geophysical reappraisal to the
1303 significance of the recent unrest at Campi Flegrei caldera (Southern Italy). *Geochemistry,*
1304 *Geophysics, Geosystems*, <https://doi.org/10.1002/2016GC006569>

1305

1306 Moretti, R., Troise, C., Sarno, F., De Natale, G., 2018. Caldera unrest driven by CO₂-induced drying
1307 of the deep hydrothermal system, *Scientific Reports* G., 8, 1, 8309.

1308

1309 Morhange, C., Marriner, N., Laborel, J., Todesco, M., & Oberlin, C., 2006. Rapid sea-level
1310 movements and noneruptive crustal deformations in the Phlegrean fields caldera,
1311 Italy. *Geology*, [34](https://doi.org/10.1130/G21894.1)(2), 93–96. <https://doi.org/10.1130/G21894.1>

1312

1313 Nespoli, F. et al., 2023. A reduced-turbulence regime in the Large Helical Device upon injection
1314 of low-Z materials powders. Nucl. Fusion, 63 076001. <https://doi.org/10.1088/174-4326/acd465>

1315

1316 Niccolini, A., 1846. La gran terma puteolana. Napoli

1317

1318 Orsi, G., De Vita, S., Di Vito, M., 1996. The restless, resurgent Campi Flegrei nested caldera (Italy):
1319 constraints on its evolution and configuration. Journal of Volcanology and Geothermal
1320 Research, 74, 3, 179–214.

1321

1322 Orsi, G., Civetta, L., Del Gaudio, C., de Vita, S., Di Vito, M. A., Isaia, R., Petrazzuoli, S.M., Ricciardi,
1323 G.P., Ricco, C., 1999. Short-term ground deformations and seismicity in the resurgent Campi Flegrei
1324 caldera (Italy): an example of active block resurgence in a densely populated area. Journal of
1325 Volcanology and Geothermal Research, 91, 2, 415–451.

1326 Osservatorio Vesuviano, 2022. Bollettino Mensile Campi Flegrei 2022 06 (In Italian).
1327 [https://www.ov.ingv.it/index.php/monitoraggio-e-infrastrutture/bollettini-tutti/mensili-dei-vulcani-](https://www.ov.ingv.it/index.php/monitoraggio-e-infrastrutture/bollettini-tutti/mensili-dei-vulcani-della-campania/flegrei/anno-2022-2/1114-bollettino-mensile-campi-flegrei-2022-06/file)
1328 [della-campania/flegrei/anno-2022-2/1114-bollettino-mensile-campi-flegrei-2022-06/file](https://www.ov.ingv.it/index.php/monitoraggio-e-infrastrutture/bollettini-tutti/mensili-dei-vulcani-della-campania/flegrei/anno-2022-2/1114-bollettino-mensile-campi-flegrei-2022-06/file)

1329

1330 Parascandola, A., 1943. Il Monte Nuovo ed il Lago Lucrino, in Bollettino della Società dei Naturalisti
1331 in Napoli, Volumi 1944–1946, 55, 151–312. Stab. tip. G. Genovese

1332

1333 Parascandola, A., 1947. I Fenomeni Bradisismici del Serapeo di Pozzuoli. Stabilimento Tipografico
1334 G. Genovese, Napoli.

1335

1336 Parmigiani, A., Huber, C., Bachmann O., 2014. Mush microphysics and the reactivation of crystal-
1337 rich magma reservoirs. JGR, <https://doi.org/10.1002/2014JB011124>

1338

1339 Pasquarè, G., Poli, S., Venzolli L., Zanchi A., 1988. Continental arc volcanism and tectonic setting
1340 in central Anatolia. Tectonophysics, 146, 217–230

1341 Rolandi, G., D'Alessio, G., Di Vito, M. (1985). Il sollevamento del suolo durante la fase preeruttiva
1342 del Monte Nuovo (Campi Flegrei). Rend. Acc., Sc. Fis. e Mat. in Napoli, 4, 52, 15 - 34

1343 Rolandi, G., Bellucci, F., Heitzler, M.T., Belkin, H.E., De Vivo, B., 2003. Tectonic controls on the
1344 genesis of the ignimbrites from the Campanian volcanic zone, southern Italy. In 'Ignimbrites of the

1345 Campanian Plain' Spec. Issue, B. De Vivo and R. Scandone Eds., Mineralogy and Petrology, 79, 3–
 1346 31

1347 Rolandi, G., De Natale G., Kilburn, C.R.J. et al., 2020a. The 39 ka Campanian Ignimbrite eruption:
 1348 new data on source area in the Campanian Plain,” in Vesuvius, Campi Flegrei, and Campanian
 1349 volcanism, Chapt. 8, B. Vivo, H. E. Belkin, and G. Rolandi, Eds., pp. 175–205, Elsevier

1350 Rolandi, G., Di Lascio, M., Rolandi, R., 2020b. The Neapolitan Yellow Tuff eruption as the source
 1351 of the Campi Flegrei caldera. in Vesuvius, Campi Flegrei, and Campanian volcanism, Chapt. 11, B.
 1352 Vivo, H. E. Belkin, and G. Rolandi, Eds., pp. 273–296, Elsevier.

1353 Rosi, M., Sbrana, A., (Eds.) 1987. Phlegrean fields (Vol. 9). Consiglio nazionale delle ricerche.
 1354

1355 Russo Mailer, C., 1979. La tradizione Medioevale dei bagni flegrei. Puteoli, studi di storia antica, III,
 1356 141-153

1357 Sabetta, F., Paciello, A., 1995. Valutazione della pericolosità sismica. La geologia di Roma- Memorie
 1358 descrittive della carta geologica d'Italia.

1359 Sacchi, M., Pepe, F., Corradino, M., Insinga, D.D., Molisso, F., Lubritto C., 2014. The Neapolitan
 1360 Yellow Tuff caldera offshore the Campi Flegrei: stratal architecture and kinematic reconstruction
 1361 during the last 15 ky. Mar. Geol. 354, 5-33

1362 Sacchi, M., Passaro, S., Molisso, F., Matano, F., Steinmann, L., Spiess, V., Pepe, F., Corradino, M.,
 1363 Caccavale, M., Tamburrino, S., Esposito, G., Vallefucio, M., Ventura, G., 2020a. The Holocene
 1364 marine record of unrest, volcanism, and hydrothermal activity of Campi Flegrei and Somma
 1365 Vesuvius. In: B. De Vivo, H.E. Belkin and G. Rolandi (Eds.) Vesuvius, Campi Flegrei, and
 1366 Campanian Volcanism, Elsevier Inc., Amsterdam, 435-469;
 1367 <https://doi.org/10.1144/GSL.SP.2006.269.01.0310.1016/B978-0-12-816454-9.00016-X>.
 1368

1369 Sacchi, M., Matano, F., Molisso, F., Passaro, S., Caccavale, M., Di Martino, G., Guarino, A., Innangi,
 1370 S., Tamburrino, S., Tonielli, R., Vallefucio, M., 2020b. Geological framework of the Bagnoli–
 1371 Coroglio coastal zone and continental shelf, Pozzuoli (Napoli) Bay. Chem. Ecol., 36, 529–549.
 1372

1373 Scandone, R., D'Amato, J., Giacomelli, L., 2010. The relevance of the 1198 eruption of Solfatara in
1374 the Phlegraean Fields (Campi Flegrei) as revealed by medieval manuscripts and historical sources.
1375 Journ. Volcanol. Geoth. Res., 189, 1–2, 202–206.

1376 Scarpa, R., Bianco, F., Capuano, P., Castellano, M., D'Auria, L., Di Lieto, B., Romano, P., 2022.
1377 Historic unrest of the Campi Flegrei caldera. In *Campi Flegrei. A Restless Caldera in A Densely*
1378 *Populated Area* (eds Orsi, G., D'Antonio, M. & Civetta, L.), 257–282.

1379 Selva, J., Orsi, G., Di Vito, M., Marzocchi, W., Sandri, L., 2011. Probability hazard map for future
1380 vent opening at the Campi Flegrei caldera, Italy. Bull. Volcanol., [https://doi.org/10.1007/s00445-011-](https://doi.org/10.1007/s00445-011-0528-2)
1381 [0528-2](https://doi.org/10.1007/s00445-011-0528-2) 1-0528-2.

1382 Somma, R., Iuliano, S., Matano, F., Molisso, F., Passaro, S., Sacchi M., Troise C., De Natale, G.,
1383 2016. High-resolution morphobathymetry of Pozzuoli Bay, southern Italy. Journ. Maps, 12, 222–
1384 230, <https://doi.org/10.1080/17445647.2014.1001800>.

1385 Soricelli, G., 2007. Comunità orientali a Puteoli. Press. Univers., Rennes, 129–144,
1386 <https://doi.org/10.4000/books.pur.6714>

1387 Sparks, S.R.J., Sigurdsson, H., Wilson, L., 1977. Magma mixing: a mechanism for triggering acid
1388 explosive eruptions. Nature, 267, 315–318

1389 Shelly, D., Hurwitz, S., 2022. Yellowstone caldera chronicles, September 5. Yellowstone Volcano
1390 Observatory, USGS ([https://www.usgs.gov/observatories/yvo/news/water-released-crystallizing-](https://www.usgs.gov/observatories/yvo/news/water-released-crystallizing-magma-can-trigger-earthquakes-yellowstone)
1391 [magma-can-trigger-earthquakes-yellowstone](https://www.usgs.gov/observatories/yvo/news/water-released-crystallizing-magma-can-trigger-earthquakes-yellowstone))

1392 Smith, V.C., Isaia, R., Pearce, N.J.G., 2011. Tephrostratigraphy and glass compositions of post-15 kyr
1393 Campi Flegrei eruptions: implications for eruption history and chronostratigraphic markers. Quat.
1394 Sci. Rev. 30, 3638–3660

1395

1396 Steinmann, L., Spiess, V., Sacchi, M., 2016. The Campi Flegrei caldera (Italy): Formation and
1397 evolution in interplay with sea-level variations since the Campanian Ignimbrite eruption at 39 ka.
1398 Journ. Volcanol. Geoth. Res., 327, 361–374

1399

1400 Strabone, 1 century BC - 1 century AD. Rerum Geogr., book V, cap. 4–5

1401

1402 Talavera Montes, A.J., 2021. Eruzioni, sismi e bradisismo nei Campi Flegrei in epoca romana tra
 1403 fonti storiche ed evidenze archeologiche e geologiche. In: *Living with Seismic Phenomena in the*
 1404 *Mediterranean and Beyond between Antiquity and the Middle Ages*, Proceedings of Cascia (25-26
 1405 October, 2019) and Le Mans (2-3 June, 2021) Conferences. Edited by Compatangelo Soussignan R.
 1406
 1407 Troise, C., Pingue, F., De Natale, G., 2003. Coulomb stress changes at calderas: modeling the
 1408 seismicity of Campi Flegrei (Southern Italy). *J. Geophys. Res.*, 108, B6, 2292,
 1409 <https://doi.org/10.1029/2002JB002006>.
 1410
 1411 Troise, C., De Natale, G., Pingue, F., Obrizzo, F., De Martino, P., Tammaro, U., Boschi, E.,
 1412 2007. Renewed ground uplift at Campi Flegrei caldera (Italy): New insight on magmatic processes
 1413 and forecast, *Geophys. Res. Lett.*, 34, L03301, doi:10.1029/2006GL028545.
 1414
 1415 Troise, C., De Natale, G., Schiavone, R., Somma, R., Moretti, R., 2019. The Campi Flegrei caldera
 1416 unrest: Discriminating magma intrusions from hydrothermal effects and implications for possible
 1417 evolution. *Earth Sci. Rev.*, 188, 108-122, <https://doi.org/10.1016/j.earscirev.2018.11.007>.
 1418
 1419
 1420 Vanorio, T., Prasad, M., Patella, D., Nur, A., 2002. Ultrasonic velocity measurements in volcanic
 1421 rocks: Correlation with microtexture. *Geophys. Journ. Intern.*, 149, 1, 22-36,
 1422 <https://doi.org/10.1046/j.0956-540x.2001.01580.x>
 1423
 1424 Vanorio, T., Virieux, J., Capuano, P., Russo, G., 2005. Threedimensional seismic tomography from
 1425 P wave and S wave microearthquake travel times and rock physics characterization of the Campi
 1426 Flegrei Caldera. *J. Geophys. Res.*, 110, 1-14
 1427
 1428 Vanorio, T., Kanitpanyacharoen, W., 2015. Rock physics of fibrous rocks akin to Roman concrete
 1429 explains uplifts at Campi Flegrei. *Science*, 349, 617–621
 1430
 1431 Varriale, I., 2004. Costa Flegrea ed attività bradisismica dall'antichità ad oggi. In *Rotte e Porti del*
 1432 *Mediterraneo dopo la caduta dell'Impero Romano d'Occidente*. IV seminario, Genova 18-19 Luglio.
 1433 De Maria L. and Turchetti R. Eds.
 1434

- 1435 Vinciguerra, S., Trovato, C., Meredith, P.G, Benson, P.M., Troise, C., De Natale, G., 2006.
 1436 Understanding the Seismic Velocity Structure of Campi Flegrei Caldera (Italy): From the Laboratory
 1437 to the Field Scale. *Pure appl. geophys.*, 163, 2205–2221, <https://doi.org/10.1007/s00024-006-0118-y>
 1438
- 1439 Wohletz, K.H., Zimanowski, B., Büttner, B.R., 2013. Magma-water interactions. in *Modeling*
 1440 *Volcanic Processes: The Physics and Mathematics of Volcanism* (Fagents, S.A., Gregg, T.K.P.,
 1441 Lopes, R.M.C. eds.) 230–257. Cambridge University Press.
 1442
- 1443 Woods, W., Cowan, A., 2009. Magma mixing triggered during volcanic eruption. *Earth and Planetary*
 1444 *Science Letters*, 288, 1–2, 30, 132-137
- 1445 Woo, J.Y.L., Kilburn, C.R.J., 2010. Intrusion and deformation at Campi Flegrei, southern Italy: Sills,
 1446 dikes, and regional extension. *J. Geophys. Res.*, 115, B12210
 1447
- 1448 Wunderman, R. ed., 2000. Global volcanism Program. Report on Hekla (Iceland). *Bullettin of global*
 1449 *volcanism network*, 25:2. Smithsonian Institution. [https:// doi org/10.5470/si](https://doi.org/10.5470/si).
 1450
- 1451 Zollo, A., Maercklin, N., Vassallo, M., Dello Iacono, D., Virieux, J., Gasparini, P., 2008. Seismic
 1452 reflections reveal a massive melt layer feeding Campi Flegrei caldera, *Geophys. Res. Lett.*, 35,
 1453 L12306, doi:[10.1029/2008GL034242](https://doi.org/10.1029/2008GL034242).
 1454
 1455
 1456

1457 **Appendix 1 - Evolution of the vertical movements involving the Via Herculea**

- 1458
- 1459 The following notes refer to the diagram represented in Fig. 3, reporting at each point the historical information
 1460 related to ground deformation in the Averno area:
 1461
- 1462 **1-** The shoreline between the cities of Baia and Pozzuoli took on a new conformation with the natural building
 1463 of a sandy coastal bar after the eruptions of Averno and Capo Miseno (5 - 3.7 ka), the last of the second post-
 1464 calderic cycle. We remember that the name *Averno* derived from the Greek *Aornon*, that is *place without*
 1465 *birds*, in reference to the presence of post-volcanic sulphurous fumes that caused the death of the birds that
 1466 flew over the waters. The dark and gloomy appearance of the landscape led the ancients to consider it the
 1467 entrance to Hades, as reported by Virgil (*Aeneid*, VI, vv 350).
 1468 We do not know precisely the time of formation of the bar structure; we can only hypothesize that it was
 1469 probably positioned between the 18th and 17th centuries BC in the coastal stretch between the cities of Baia

1470 and Pozzuoli, with a height of about 6 m, like the other coastal bars formed more recently in nearby areas,
1471 where the seabed has a depth of about 6-7 m. The formation of the sea barrier blocked a portion of the sea
1472 inside the inlet, which took the shape of a lake (Fig. 2a and Fig. 4).

1473

1474 **2-** This point can be traced back, from a historical and chronological point of view to the 8th century BC. In
1475 the diagram it is positioned at approximately 5 m above sea level, suggesting a subsidence of the coastal bar
1476 of about 2 m from the previous point. In fact, from a writing by Diodorus Siculus (Book IV) we know that:..
1477 ***this dam was continually invaded and ruined by the stormy sea, which often made it impassable...*** It is known
1478 from coastal dynamics studies that waves breaking against a dam, placed above a seabed 7 m deep, reach a
1479 height equal to 3/4 of the depth of the same seabed, in this case approximately 5 m, i.e., a height equal to the
1480 barrier above the sea level. Therefore, the via Herculea, hit by violent waves, constituted an impassable road
1481 for the inhabitants of Cuma to reach the lands they cultivated in the surroundings of Pozzuoli, which, starting
1482 from the 8th century, took the name of Via Herculea (Fig. 2b and Fig. 4). Finally, the hypothesis of a height
1483 of 5 m, as resulting from submersion started since the 17th century BC, seems likely.

1484

1485 **3- 4 -** The body of water formed by the coastal bar, in the 1st century BC, was owned by Sergio Orata. The
1486 lake, making generous profits from fish farming, was named "*Lucrino*", derived from the Latin *Lucrum* (profit)
1487 (Fig. 2c). The owner, around 60 BC, to protect his interests turned directly to the Roman Senate to have the
1488 Via Herculea repaired, because at that time, being at a height of about 2 m above sea level, it had almost been
1489 destroyed by the waves that crossed it, preventing him from practicing his lucrative fish farming business
1490 (point 3). The Senate appointed Julius Caesar, who in 59 BC built a breakwater barrier, located outside the
1491 dam towards the open sea (*Opus Pilarum*). He also ordered the installation of canals closed by opening
1492 platforms (*Claustre*). Julius Caesar's project defended the Via Herculea essentially from the horizontal force
1493 exerted by violent wave motion, not understanding the effect of subsidence. In 37 BC, general Agrippa, by
1494 order of Octavian, engaged in the naval war against Pompeo Sextus, chose the coastal sector between the lakes
1495 Lucrino and Avernus for the construction of a new military port system, called *Portus Julius*. A new main
1496 entrance was built, consisting of a canal with two long banks in '*opus pilarum*', cutting and equipping the Via
1497 Herculea with a mobile bridge, to access its interior, while at the same time widening the narrow opening that
1498 connected the Averno and Lucrino lakes to allow access of large ships in the shipyard (Fig. 2c). Furthermore,
1499 Agrippa reinforced the Via Herculea and added piers, supported by orthogonal pillars and having also sensed
1500 a problem of subsidence,... ***raised its level (Strabone, 1 century BC-1 century AD)*** (point 4).

1501

1502 **5- 6 -** The abandonment of Portus Julius by the Roman fleet, starting from 12 BC, as well as of the remaining
1503 part of Lake Lucrino, due to the impossibility of continuing fish farming, was the result of the continuing
1504 subsidence, which, according to Aucelli et al. (2020), between 37 BC and the beginning of the 1st century AD
1505 further accelerated.

1506 In the 5th century AD the dam, few meters above sea level (point 5), was also damaged by a violent sea storm.
1507 An attempt to restore the dam again was made by Theodoric, regent of the Ostrogothic kingdom in Italy from
1508 493 AD, who decided, in 496 AD, to repair the damage and probably also raised its level (*Cassiodorus, Varia,*
1509 *Book I*) (point 6). This can be also deduced from the fact that Lake Lucrino was still well identified in 522
1510 AD (G.C. Capaccio - Puteolana historia, in Parascandola 1943).

1511

1512 **7-8** - Around the second half of the 6th century (556 AD), some fishermen attempted to reactivate fish farming
1513 in Lake Lucrino, but the dam soon could not guarantee an adequate yield, because it had reached a height of
1514 just a few meters above sea level (point 7), not allowing fish farming (Parascandola, 1943).

1515 As we will show in Appendix-2, historical documents indicate that, at the lower city around Pozzuoli, the
1516 famous Serapeo (Macellum) began the phase of submersion below sea level in the 4th-5th century AD. At the
1517 area facing the Avernus, the above historical documents indicate that the submersion most likely occurred
1518 between the 6th and 7th centuries AD. This could be related to either height increasing interventions and /or
1519 to a lower speed of subsidence at the site of Via Herculea, as compared to the Serapeo.

1520

1521 **9** – In the 14th century we have evidence of the submersion through the writings of Petrarca and Boccaccio.
1522 Below we will report some sentences from the two poets, giving indications on the subsidence in this period
1523 (Parascandola 1943):

1524 - Petrarca, who lived in Naples in 1341, visited the coastal area of Avernus, (...*I then saw the places of*
1525 *Avernus and Lucrino..... and the superb road of Gaius Caligula now swallowed up by the waves..... Note*
1526 *that Opus Pilarum mistakenly believed to be the road of Caligula*). From this observation we deduce that
1527 Opus Pilarum was submerged in the 14th century (Fig. A1). From the same observation it further seems likely
1528 that, since the 4-5 m high pylons, submerged for a couple of metres, are not visible, and given the pylons were
1529 higher than Via Herculea of about 3 meters, the already submerged Via Herculea should have been submerged
1530 at that time for about 5-6 m.

1531 - Boccaccio came to Naples in 1348 and, after visiting the Averno area, he clearly expressed the concept,
1532 although indirectly, that Lake Lucrino was not recognized as it was invaded by the sea, mixing with the waters
1533 of Avernus (...*to Avernus, connected in ancient times with the nearby lake Lucrino where it recalls the*
1534 *waters of portus Iulius*: Boccaccio, 1355-1373).

1535 Boccaccio noted that, since there was no barrier on the Via Herculea which formed the Lucrino, the rough sea
1536 even broke into Lake Averno. Therefore, we can undoubtedly say that in the 14th century via Herculea was
1537 completely submerged and Lake Lucrino disappeared because it was invaded by the sea.

1538

1539 **10** - As we will demonstrate later, in the 15th century the ground movements of the Campi Flegrei area changed
1540 from subsidence to uplift. The uplift began, the actual amount of which in the Averno area can be only given
1541 in an approximate but equally significant way, because it is ascertained, from the writings of all the chroniclers
1542 of the time (see Parascandola, 1943) that the Via Herculea did not re-emerge in this period (fig 2d). What is

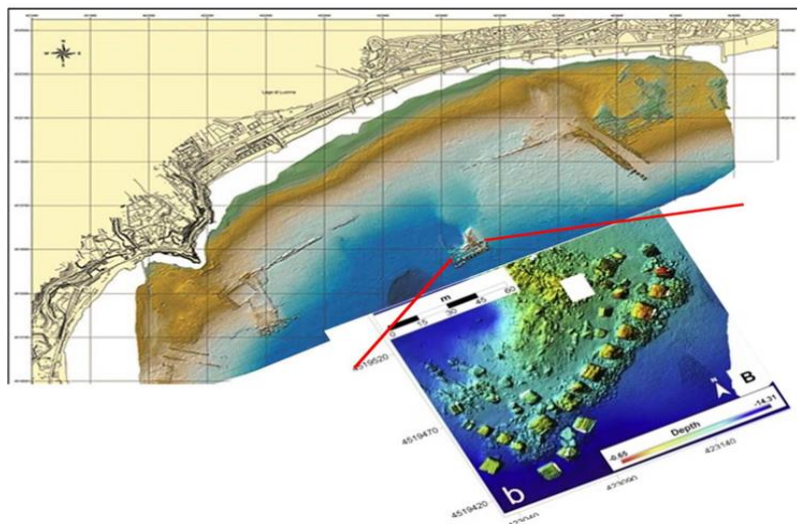
1543 reported by the historian San Felice is almost common to all the chroniclers: *The sea had taken possession of*
 1544 *Lucrino, so that the name could no longer be given to the ancient lake.*
 1545

1546

1547 **Fig. A1 - The remains of the Via Herculea currently located at 4-5m bsl, with the columns of Opus**
 1548 **Pilarum approximately 300m away in the open sea. An enlargement of the structure of Opus Pilarum is**
 1549 **also reported**

1550 Shortly before the eruption, the general caldera uplift was also accompanied by a localized uplift of the area
 1551 where Monte Nuovo would have risen shortly after, in 1538, located in close contact with the Lucrino basin
 1552 (Fig. 2d). Such a local uplift was estimated at about 7 m (Parascandola, 1943), so the Via Herculea would
 1553 certainly have emerged if it had been close to the sea surface at the end of the 15th century. A significantly
 1554 larger uplift, of 19 m as hypothesized by Di Vito et al (2016), can be certainly ruled out from the observation
 1555 that Via Herculea did not reemerge.

1556 The topic of the local uplift before eruption is relevant, so we insist on other aspects linked to the entire area
 1557 buried by the products of 1538 Monte Nuovo eruption. Until a short time before the eruptive event, two small
 1558 tuff hills, called *Montagnella* and *Monticello del Pericolo* (Parascandola, 1936), overlooked the Averno Bay,
 1559 above which the *village of Tripergole* extended. This village, thanks to the Angevins, developed with the
 1560 construction of a hospital with 30 beds, to access the numerous springs and thermal facilities available to the
 1561 hospitalized patients, with an adjoining pharmacy. Ancient buildings used for thermal baths (*Trugli*) present
 1562 in the Tripergole area were highly compromised between the end of the 15th century and the beginning of the
 1563 16th, when the Pozzuoli area was hit by major earthquakes. The earthquakes caused extensive damage to the
 1564 thermal health and ecclesiastical buildings of Tripergole, but not so devastating than expected if a ground uplift
 1565 about 20 m high would have occurred. Also the so-called *Temple of Apollo*, still present along the north-
 1566 eastern bank of the Averno lake (Fig. A2), testifies against a so large and sudden uplift. The structure is an
 1567 imposing building identified as a grandiose thermal room, covered by a dome, now partly collapsed, which
 1568 measured approximately 38 metres in diameter, built in the 1st century AD to exploit a series of hydrothermal



1569 springs along the eastern side of Avernus, then expanded with the large octagonal hall (the one that is still
1570 visible) in the following century. This structure was identified by Biondo da Forlì as the bathroom of Cicero
1571 (Lanzarin, 2021), that, due to its particular location protected by the Averno crater belt, was not involved in
1572 the burial of the *Monticello del Pericolo*, the *Montagnella* and the village of *Tripergole*, with its renowned
1573 thermal baths.

1574



1575

1576 **Fig. A2 – The so-called Temple of Apollo on the east bank of the Avernus. You can see the remains of a**
1577 **circular building with a "cap" vault, which later collapsed, typical of a "Truglio", i.e. a spa building**
1578 **(internet source)**

1579

1580

Appendix 2 - Evolution of the ground movements involving the Pozzuoli area

1581

1582 Phases of submersion during the Greek age have been detected in the Pozzuoli area by Gauthier (1912),
1583 specifically in the eastern sector of Agnano. The author discovered Greek walls beneath the ruins of Roman
1584 baths which were restored in the 6th century AD. These, in turn, underlie lacustrine sediments that filled an
1585 ancient lake originally existing within the Agnano crater. However, the most evident subsidence phases have
1586 been recorded since Roman times, by the structures of the so-called Temple of Serapis in Pozzuoli. Built in
1587 the 2nd century AD and restored and completed in the 3rd century AD, during the Severan era, this structure
1588 exhibits the typical architecture of a Roman market ("Macellum").

1589 To determine whether the construction preceding the 2nd century AD had a connection with a temple, we must
1590 go back to 105 BC, when a contract was stipulated between the municipality of Pozzuoli and a college of
1591 builders for repairs of public buildings (lex parieti faciundo). Among these was the Ades Serapis (Parascandola
1592 1947), indicating that a temple dedicated to Serapis, (an Alexandrian deity often regarded as protector of
1593 merchants and sailors) existed during this period. By the end of the 2nd century BC, the cult of Serapis had
1594 spread throughout the Mediterranean and its sanctuaries, as well as those of other Egyptian deities, were
1595 frequented by Roman-Italics. It is probable, therefore, that the introduction of the cult of Serapis in Puteoli is
1596 related to the presence of an Egyptian community in the Puteolan port (Soricelli 2007). It is important to try to

1597 establish the relationships between this building and the Macellum built later, specifically whether the Ades
1598 Serapis could have an ancestral link with a more recent cult building, that was then transformed into a typical
1599 Roman market. This relationship is suggested by the discovery of a statue of Jupiter Serapis during the
1600 excavations of the Macellum in 1750 (see below). However, data reconstructed by Amato and Gialanella
1601 (2013; Fig.3), indicate that the first floor present in the substrate below the Macellum dates from the Flavian
1602 period (69 -96 AD). The finds in the reworked pyroclastic materials which are 4 meters thick below the first
1603 floor indicate a chronological interval between the end of the Republic and the beginning of the Empire (44
1604 BC - 14 AD). This suggests that the Ades Serapis was likely built in a different position from the macellum,
1605 with which it therefore has no ties. The architectural elements of Macellum are part of the restoration works
1606 carried out on the Serapeo during the Severan Age (194 - 235 AD), with the installation of the 4th floor around
1607 230 AD, located approximately 2 m above the 3rd floor. The existing structure (Fig. 6), still present in the
1608 same area today, provides important evidence for reconstructing the ground movements. These movements
1609 can be identified in:

1610 *The marble floor of the macellum (4th floor; see also Fig. A3b);

1611 * The height of the three columns of the pronaos (12.70 m high, with the first 6.2 m displaying a 2.70m band
1612 perforated by lithophagus colonies (Fig. A3).

1613 The historical information about the ground movements, is schematized in Fig. 6 of the main text, as follows:

1614 **1** - In the 2nd century AD the 3rd floor of the Serapeum reached approximately 1m above sea level. It was
1615 sporadically invaded by the sea, to the point that, it was considered appropriate to build a 4th floor in 230 AD,
1616 located at 2m above sea level.

1617

1618 **2** - The flooding progressively affected the coast, leading to the transfer of ships from the port of Puteoli to
1619 Constantinople in 325-330 AD (Gianfrotta 1993). It is important to highlight that the 4th floor was invaded
1620 by the sea in 394 AD. The bank was restored on the left side and the right side of the macellum, in the area
1621 where structures functional to the port and the emporium were located, and to protect it from the sea waves
1622 with the construction of coastal embankments. These important works were supervised by the Campanian
1623 Consul Valerius Hermonius Maximus (Camodeca 1987, Caruso 2004).

1624

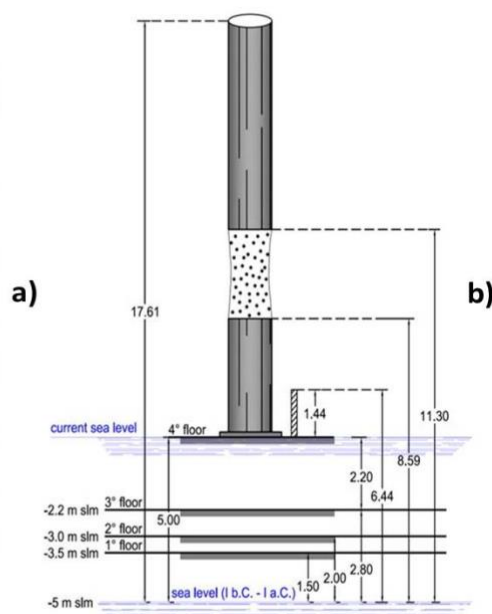


Fig. A3 – a) Macellum showing pronao columns, b) Floors underlying columns

1625

1626

1627

1628 **3** - In the 6th-7th century, the citizens who had completely depopulated the lower part of Pozzuoli felt the need
 1629 to take refuge in a sort of fortified citadel (castrum), equipped with a drawbridge, giving rise to the Acropolis
 1630 of the Rione Terra (Varriale, 2004).

1631

1632 **4** - In the 9-10th century, according to Parascandola (1947), the maximum submersion of the 4th floor of the
 1633 Serapeum occurred. Due to the subsidence of the Pozzuoli area, between the 8th and 10th centuries, the Agnano
 1634 Plain, immediately east of Pozzuoli, was invaded by water for the stagnation of thermal and rainwater,
 1635 transforming it into a lake (Annechino, 1931).

1636

1637 **5 -7** - In such a context, the most critical periods of the submersion phase occurred. The sea increasingly
 1638 surrounded the Rione Terra, that appeared like a medieval village, with a drawbridge at the entrance to the
 1639 cliff. The same context was depicted in the 11th century by the Arab geographer *Idrisi* in his *Opus*
 1640 *Geographicum*, describing Pozzuoli as a "*castle*" (Varriale, 2004).

1641 In the 12th century subsidence was still active. A writing deriving from an account of Benjamin ben Yonah
 1642 de Tudela who, visiting the Jewish communities of the Mediterranean, passing through Pozzuoli, described:
 1643 *turres et fora in aqua demersa quae in media quondam fuerant* (Russo Mailer C. 1979, Caruso 2004). The
 1644 Pozzuoli district continued to subside in the 13th century, as can be deduced from an account written in 1251
 1645 by the historian Niccolò Jamsilla (*Historia de rebus gestis Frederici II imperatoris ejusque filorum*
 1646 *Corradiet Manfredi Apuliae et Siciliae regnum*) describes the places between Agnano and Pozzuoli as
 1647 follows: ...*videlicet Putheolum mari mantibusque inaccessibilius circumquaque conclusum*... (Fuiano
 1648 1951).

1649 In essence, what was observed by the Arab geographer Idris in the 11th century, was also written by the
 1650 historian Jamsilla in 1251, confirming that Rione Terra "was *an unapproachable mountain completely*

1651 *surrounded by the sea*". This highlights that, over more than 3 centuries, the sea level rose due to subsidence
1652 of the tuffaceous walls of the Rione Terra.

1653

1654 **8** – Further eyewitness accounts from by Boccaccio, who lived in Naples between 1327 and 1341, reported that
1655 a fisherman's wharf in the Bay of Pozzuoli became completely submerged (Mancusi, 1987). This document
1656 supports the description of the lower part of the city being completely submerged.

1657

1658 **9-10** – A gouache from 1430, known as *Bagno del Cantariello*, part of the famous Balneis Puteolanis of the
1659 Edinburgh Codex (Di Bonito & Giamminelli, 1992) indicates the complete submergence of the 4th floor of
1660 the Serapeum by at least 10 meters. (Fig. 7). This context is supported by a description from 1441 indicating
1661 that in 1441 "*the sea covered the littoral plain, today called Starza*" (De Jorio, 1820; Dvorak and
1662 Mastrolorenzo, 1991) (see Fig. 8).

1663 For a more precise description of this morphological context, it is useful to refer to the excavation of the
1664 Serapeum carried out in 1750, when this monument was freed from the blanket of sediments that buried it (see
1665 Fig. 12), made up of approximately 8 m of filling sediments, plus two meters of deposits from the pyroclastic
1666 flow of the M. Nuovo eruption. By replacing the latter materials with the approximately 2 m blade of sea water
1667 in the 1430 scenario (Fig. 7c), we arrive at the landscape picture in Fig. 7a, exemplified in Fig. 8d.

1668

1669 **Appendix 3 - Comparing past and recent earthquakes: from intensity to magnitude**

1670 To better compare the past **earthquakes** with the recent and present-day seismicity recorded at Campi
1671 Flegrei we must convert intensities in magnitude. In Fig. 19, we present a tentative correlation
1672 between the epicentral intensity (I_0) and the magnitude (M_L). Choosing the correct relation between
1673 I_0 and M_L is not straightforward, particularly in this case involving peculiar volcano-tectonic
1674 earthquakes. Nonetheless, it is important to establish such a relation to compare the seismicity
1675 observed during the 1430-1582 period, as inferred by Guidoboni and Cucciarelli (2011), with the
1676 seismicity experienced during the recent unrests. To determine the I_0 - M_L relation, we are confident
1677 that, despite the availability of several formulas in the literature, the best approach is to consider a
1678 precise geographical and seismotectonic context, especially in a volcanic setting. Different features
1679 allow to discriminate between volcanic and tectonic earthquakes, which suggests caution in using
1680 correlations derived from tectonic areas for volcanic earthquakes, and vice versa (Milana et al., 2010).
1681 In order to build a realistic relation between seismic intensity and magnitude in this area, we utilized
1682 the computed intensities of two earthquakes that occurred in the Campi Flegrei region in 1983
1683 (Branno et al., 1984; Marturano et al., 1988; Milana et al., 2010; Charlton et al., 2020), during the
1684 previous unrest of 1982-1984 (Troise et al., 2019). Additionally, we considered a $M=5.0$ earthquake
1685 that occurred in the similar volcanic area of Colli Albani (Sabetta and Paciello, 1995). The $M=4.0$
1686 earthquake occurred on October 4, 1983, at Campi Flegrei, was found to have a maximum intensity

1687 I_0 =VII (Branno et al., 1984; Marturano et al., 1988). An earthquake of magnitude $M=3.5$, which
1688 occurred in the same swarm on October 4, 1983, was found to have a maximum intensity I_0 =V (Fig.
1689 19: Marturano et al., 1988). Furthermore, Sabetta and Pugliese (1995) reported an earthquake of
1690 $M=5.0$, with a maximum magnitude I_0 =VIII.

1691 These correlations between intensity and magnitude were utilized to assign realistic magnitude values
1692 to the macroseismic intensities deduced from the analysis of historical seismicity (Guidoboni and
1693 Cucciarelli, 2011), as shown in Fig. 19. They were also used to transform the magnitude of
1694 earthquakes associated with recent unrest phases into macroseismic intensities, as we will discuss
1695 later.

1696

1697

1698

1699

1700

1701

1702

1703

1704

1705

1706

1707

1708

1709

1710

1711

1712

1713